Control of Dispersity and Stereochemistry in Free Radical Telomerizations: A Radical Addition, Cyclization, Chain Transfer (ACT) Strategy†

Ned A. Porter,* Gregory S. Miracle, Scott M. Cannizzaro, Randall L. Carter, Andrew T. McPhail, and Lin Liu

Contribution from the Department of Chemistry, Duke University, Durham, North Carolina 27708

Received April 21, 1994®

Abstract: A general strategy for the stereoselective preparation of $n = 2$ telomers displaying narrow dispersity is reported. Covalent assemblies composed of a rigid base compound, flexible tethers, and oxazolidine acrylamide monomers were reacted under free radical conditions to afford macrocyclic precursors to the targeted telomers through an addition, cyclization, chain transfer (ACT) sequence. Subsequent hydrolysis and esterification afforded the desired products with excellent stereoselectivity and teloselectivity. Systematic variation of system components (the rigid base compound, the functionality linking base compound to the tethers, the length of the tethers, the configuration at the site of oxazolidine attachment, and the auxiliary blocking group) allowed for identification of the structural elements necessary for successful implementation. It was found that each of these variables had a marked influence on the performance of the covalent assembly.

Many synthetically interesting target molecules contain skeletal fragments that are comprised in part of a finite number of repetitive chiral segments. Examples containing multiple consecutive propionate units include (–)-lardolure **1**, the aggression pheromone of the acarid mite *Lardoglyphus konoi*,[1] and **2**, a compound isolated from the preen-gland wax of the domestic goose *Anser a.f. domesticus*.[2]

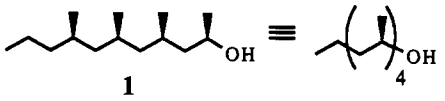

1

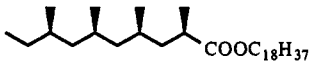

2

The occurrence of repetitive chiral units is, of course, not limited to the propionate fragment. Isotactic permethylated polyols have been isolated from a variety of toxin-producing blue-green algae, for example, and polyols with repetitive structures are also known and have been the focus of synthetic investigations.[3]

Linear synthetic approaches using established methodologies have been utilized to construct structures such as those illustrated above.[4] While conventional methodology has in many instances succeeded in obtaining high degrees of stereoselectivity, the approach to repetitive substructures suffers with respect to overall efficiency. For iterative strategies that require multiple protection and deprotection of labile functional groups and recursive adjustments in oxidation state, even in cases where such manipulations are high yielding, the shear number of transformations inevitably take their toll. Acceptable yields notwithstanding, there is still an equally important efficiency issue: time management, since multistep synthetic sequences can be slow.

One of the salient features of free radical addition reactions is their ability to construct multiple carbon–carbon bonds in a single reaction. This powerful feature would seem to make them ideally suited to the synthesis of the kind of repetitive fragments shown above. Indeed, chemists have pursued this option, but their efforts to exploit this trait have been hampered by two overriding limitations: (1) lack of stereochemical control and (2) an inability to control adequately the number of addition reactions that occur. In the last few years, understanding has progressed to the point that the first limitation can be overcome. Given that, we set out to develop a rational strategy that would overcome both limitations and allow for the use of free radical addition reactions to construct repetitive chiral fragments in a single step.

Strategies that simplify telomer distribution have been reported by several groups.[5] Simple alteration of the monomer/chain transfer reagent feed ratio provides some measure of control, albeit crude, over the dispersity of free radical telomerization reactions. The degree of control, however, is entirely unsatisfactory from a synthetic standpoint for all but the lowest telomers.

† Taken in part from the Dissertation of G. S. Miracle, Duke University, 1993.

• Abstract published in *Advance ACS Abstracts*, September 15, 1994.

(1) (a) Kuwahara, Y.; Yen, L. T. M.; Tominaga, Y.; Maysumoto, K.; Wada, Y. *Agric. Biol. Chem.* **1982**, *46*, 2283. For the stereochemistry of lardolure, see: (b) Mori, K.; Kuwahara, S. *Tetrahedron* **1986**, *42*, 5545. For syntheses, see: (c) Kaino, M.; Naruse, Y.; Ishihara, K.; Yamamoto, H. *J. Org. Chem.* **1990**, *55*, 5814. (d) Mori, K.; Kuwahara, S. *Liebigs Ann. Chem.* **1987**, 555. (e) Mori, K.; Kuwahara, S. *Tetrahedron* **1986**, *42*, 5539.

(2) (a) Odham, G. *Ark. Kemi* **1963**, *21*, 379. (b) Murray, K. E. *Aust. J. Chem.* **1962**, *15*, 510. (c) Weitzel, G.; Fretzdorff, A.-M.; Wohjan, J. *Hoppe-Saylers Z. Physiol. Chem.* **1952**, *291*, 46.

(3) (a) Kikuzaki, H.; Tsai, S.-M.; Nakatani, N. *Phytochemistry* **1992**, *31*, 1783. (b) Nakata, T.; Hata, N.; Iida, K.; Oishi, T. *Tetrahedron Lett.* **1987**, *28*, 5661. (c) Mynderse, J. S.; Moore, R. E. *Phytochemistry* **1979**, *18*, 1181. For syntheses and stereochemistry, see: (d) Mori, Y.; Kohchi, Y.; Suzuki, M. *J. Org. Chem.* **1991**, *56*, 631. (e) Rychnovsky, S. D.; Griesgraber, G. *J. Org. Chem.* **1992**, *57*, 1559. (f) *Antibiotics, Chemotherapeutics, and Antibacterial Agents for Disease Control*; Grayson, M., Ed.; Wiley: New York, 1982; pp 275–301. (g) Lipshutz, B. H.; Kotsuki, H.; Lew, W. *Tetrahedron Lett.* **1986**, *27*, 4825, and references cited therein. (h) Rychnovsky, S. D.; Rodriguez, C. *J. Org. Chem.* **1992**, *57*, 4793. (i) Kim, Y. J.; Furihata, K.; Shimazu, A.; Furihata, K.; Seto, H. *J. Antibiot.* **1991**, *44*, 1280.

(4) See, for example: (a) Seebach, D.; Maestro, M. A.; Sefkow, M.; Neidlein, A.; Sternfeld, F.; Adam, G.; Sommerfeld, T. *Helv. Chim. Acta* **1991**, *74*, 2112. (b) Evans, D. A.; Nelson, J. V.; Taber, T. R. *Topics Stereochemistry* **1982**, *13*, 1, and references cited therein. (c) For a review of the synthesis of 1,3-polyols, see: Oishi, T.; Nakata, T. *Synthesis* **1990**, 635. (d) For an approach utilizing thermodynamic equilibration of multiple stereocenters, see: Zhao, Y.-b.; Pratt, N. E.; Heeg, M. J.; Albizati, K. F. *J. Org. Chem.* **1993**, *58*, 1300.

(5) For a historical perspective, see: Miracle, G. S.; Cannizzaro, S. C.; Porter, N. A. *ChemTracts* **1993**, 147.

0002-7863/94/1516-10255$04.50/0 © 1994 American Chemical Society

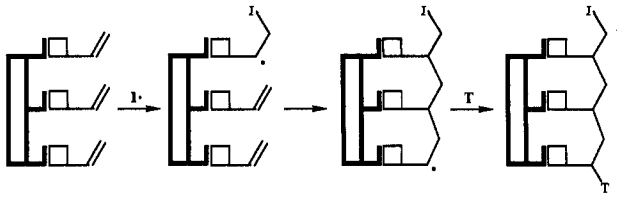

Figure 1. The template approach to an $n = 3$ telomer. Boxes represent chiral auxiliaries linking the alkenes to the template (bold).

To gain sufficient control, systems must be designed that delay introduction of the chain transfer event until a specified number of chain growth steps have occurred. The goal is to develop stratgies that maximize the chain transfer coefficient for the desired telomer while minimizing it for all others. A given chain transfer coefficient may be maximized through an increase in the rate of chain transfer or through a decrease in the rate of chain growth. This challenge has been approached by two complementary methods, both of which utilize dilution to afford a relative rate enhancement for a desired intramolecular reaction over competing intermolecular reactions.

For cases where the chain transfer agent is located on the growth chain, a geometric constraint must be introduced that prohibits an intramolecular chain transfer event from occurring prematurely. This may be accomplished by attaching initiating and terminating functionalities at a fixed distance along a rigid framework. The distance between the two defines the optimum number of chain growth events that must occur before the span is traversed and unimolecular chain transfer becomes feasible. This elegant method for controlling telomer distribution was pioneered by Feldman,[6] who suggested the term *oligoselectivity* to describe such discriminating processes.

A second strategy for control of telomer dispersity involves attachment of monomers to a template and utilizes cyclotelomerization in competition with intermolecular chain transfer, see Figure 1. Except for the initial contributions of Kämmerer,[7] cyclotelomerization has seen limited use. Nevertheless, reports of cyclotelomerization[8] and cyclopolymerization,[9] along with systematic investigations of radical macrocylization,[10] make this approach to the control of oligomer dispersity potentially attractive. The ability to rely on closure of large rings allows for the possibility of incorporating several key structural elements into the template. We report here the results of studies that systematically examine these important template structural elements.[11]

Scheme 1. Synthesis of First Generation Covalent Assembly **4** and Model Compounds[a]

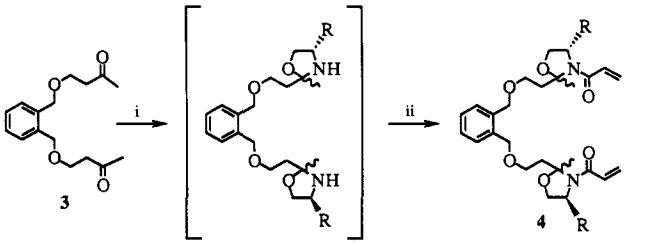

[a] (i) *S*-valinol or *S*-*tert*-leucinol, CH_2Cl_2, $MgSO_4$ and (ii) acryloyl chloride, *N*-methylmorpholine, catalyst DMAP.

Scheme 2. Chemistry of the ACT reaction on Template 4

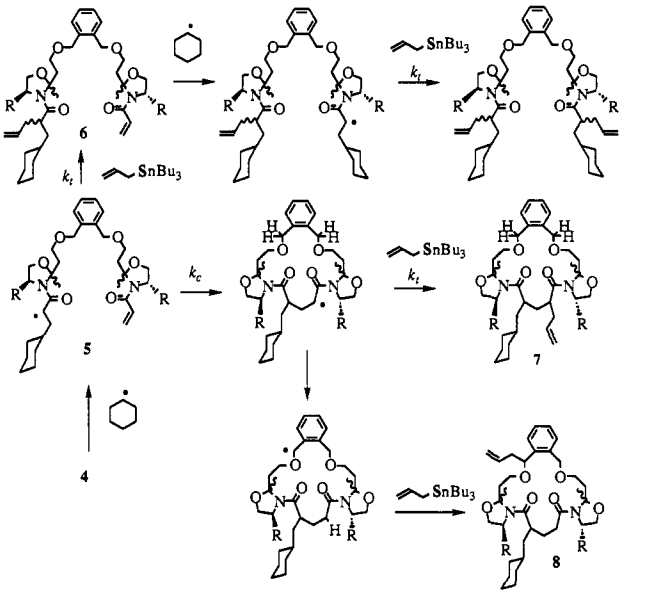

Results and Discussion

First Generation Templates. The first generation covalent assembly was prepared according to Scheme 1. Bisketone **3** was reacted with (*S*)-valinol or (*S*)-*tert*-leucinol to form an intermediate bisoxazolidine that was not isolated but rather was acylated *in situ* with acryloyl chloride to obtain the covalent assembly **4** (55%) as an inseparable mixture of diastereomers.

Given our objectives, the choice of a reaction to which **4** would be subjected is reasonably straightforward. The alkyl iodide/allyltributyltin system seems ideal for several reasons.[12] Transfer of an allyl group not only assures the formation of a new stereocenter but also provides functionality amenable to a wide variety of further synthetic transformations. Since addition of intermediate radicals to allyltributyltin is expected to be slower than to acrylamide, a rapid cyclization step is not required.[13] This ability to provide for relatively long lifetimes of intermediate radicals is an attractive feature since rates of free radical macrocyclization are moderate, usually in the range of 10^4 s^{-1}.[8]

Reaction of **4** with cyclohexyl iodide/allylstannane is expected to give a complex mixture of products. The starting material is a mixture of isomers at each oxazolidine quaternary carbon, and a radical addition/cyclization/allyl transfer sequence would introduce two additional stereogenic centers in the expected macrocyclic products **7**, see Scheme 2. Initial success was achieved

(6) (a) Feldman, K. S.; Lee, Y. B. *J. Am. Chem. Soc.* **1987**, *109*, 5850. (b) Feldman, K. S.; Bobo, J. S.; Ensel, S. M.; Lee, Y. B.; Weinreb, P. H. *J. Org. Chem.* **1990**, *55*, 474. (c) Feldman, K. S.; Bobo, J. S.; Tewalt, G. L. *J. Org. Chem.* **1992**, *57*, 4573.

(7) (a) Kämmerer, H.; Ozaki, S. *Makromol. Chem.* **1966**, *91*, 1. (b) Kämmerer, H.; Jung, A. *Makromol. Chem.* **1967**, *101*, 284. (c) Kämmerer, H.; Jung, A.; Shukla, J. S. *Makromol. Chem.* **1967**, *107*, 259. (d) Kern, W.; Kämmerer, H. *Pure Appl. Chem.* **1967**, *15*, 421. (e) Kämmerer, H.; Önder, N. *Makromol. Chem.* **1968**, *111*, 67. (f) Kämmerer, H.; Shukla, J. S. *Makromol. Chem.* **1968**, *116*, 62. (g) Kämmerer, H.; Shukla, J. S.; Scheuermann, G. *Makromol. Chem.* **1968**, *116*, 72. (h) Kämmerer, H.; Hegemann, G. *Makromol. Chem.* **1970**, *139*, 17. (i) Guéniffey, H.; Kämmerer, H.; Pinazzi, C. *Makromol. Chem.* **1973**, *165*, 73. (j) Kämmerer, H.; Hegemann, G. *Makromol. Chem.* **1982**, *183*, 1435. (k) Kämmerer, H.; Hegemann, G. *Makromol. Chem.* **1984**, *185*, 635.

(8) Shea, K. J.; O'Dell, R.; Sasaki, D. Y. *Tetrahedron Lett.* **1992**, *33*, 4699.

(9) (a) Wulff, G. In *Recent Advances in Mechanistic and Synthetic Aspects of Polymerization*; Fontanille, M., Guyot, A., Eds.; D. Reidel: Boston, 1987; p 399. For earlier examples of achiral cyclocopolymerizations, see: (b) Polowinski, S. *Polimery* **1972**, *17*, 409. (c) Polowinski, S.; Janowska, G. *Polimery* **1972**, *17*, 464. (d) Polowinski, S.; Janowska, G. *Eur. Polym. J* **1975**, *11*, 183.

(10) (a) Porter, N. A.; Magnin, D. R.; Wright, B. T. *J. Am. Chem. Soc.* **1986**, *108*, 2787. (b) Porter, N. A.; Chang, V. H.-T. *J. Am. Chem. Soc.* **1987**, *109*, 4976. (c) Porter, N. A.; Chang, V. H.-T.; Magnin, D. R.; Wright, B. T. *J. Am. Chem. Soc.* **1988**, *110*, 3554. (d) Porter, N. A. Stereochemical and Regiochemical Aspects of Free Radical Macrocyclizations. *Organic Free Radicals*; Proceedings of the Fifth International Symposium; Fischer, H., Heimgartner, H., Eds.; Springer-Verlag: Berlin, 1988; p 187.

(11) A preliminary report of this work has been published. Miracle, G. S.; Cannizzaro, S. M.; Porter, N. A. *J. Am. Chem. Soc.* **1992**, *114*, 9683.

(12) Curran, D. P. *Synthesis* **1988**, 417 and 489.

(13) For an example of a cyclization/transfer sequence using allyltri-*n*-butylstannane, see: Moriya, O.; Kakihana, M.; Urata, Y.; Sugizaki, T.; Kageyama, T.; Ueno, Y.; Endo, T. *J. Chem. Soc., Chem. Commun.* **1985**, 1401.

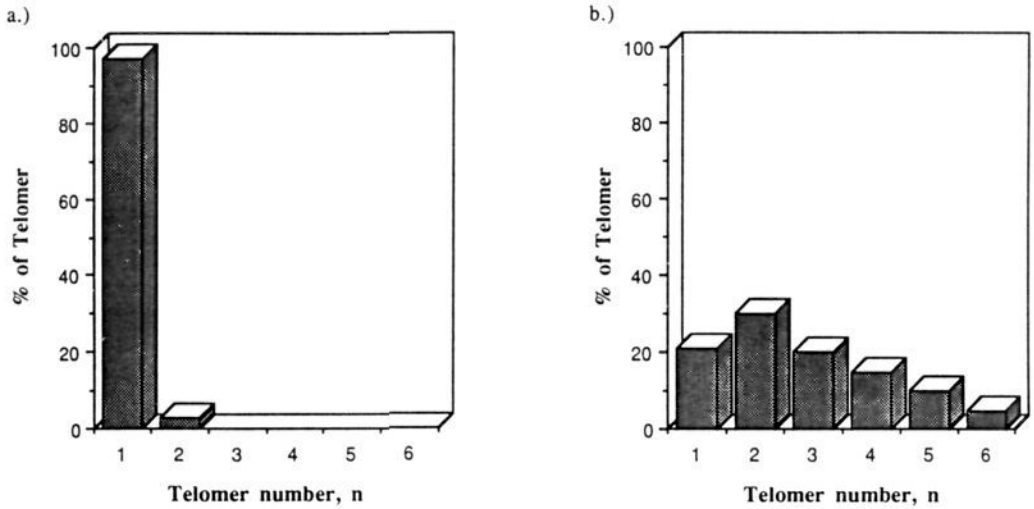

Figure 2. Product histogram for methyl acrylate telomerization: (a) 5 mM methyl acrylate, 80 mM cyclohexyl iodide, 400 mM allyltributylstannane and (b) 500 mM methyl acrylate, 120 mM cyclohexyl iodide, 300 mM allyltributylstannane.

using thermal (AIBN) initiation in refluxing benzene with concentrations of 10 mM **4**, 80 mM cyclohexyl iodide, and 200 mM allyltributyltin. The course of the reaction was followed by monitoring the disappearance of **4** and the appearance of products **7** by gas chromatography. In optimizing the ACT reaction, varying concentrations of covalent assembly **4**, cyclohexyl iodide, and allyltributyltin were employed. The best yield of macrocycle for these first generation templates (45%) was obtained using 5 mM **4**, 80 mM cyclohexyl iodide, and 400 mM allyltributyltin.

A complication that surfaced during the course of this work (*vide infra*) was the possibility of hydrogen atom abstraction either preceding or following cyclization but preceding final chain transfer. For attack at the distal benzylic position (as illustrated in Scheme 2), this is simultaneously a 1,10- and a 1,11-abstraction. For proximal attack, 1,8- and 1,13-processes are involved. Radicals formed by H-atom transfer may in turn undergo chain transfer to afford products such as **8**, Scheme 2.

Development of an Assay for Product Telomers. The crude ACT reaction mixture was concentrated, and the bulk of the tin products were removed through chromatography and KF treatment. The mixture, containing adducts **7** and **8** among others, was then hydrolyzed under acidic conditions[14] to yield the acrylic acid telomers of general structure **9**. The mixture of acids was treated with base, washed with ether, reacidified, and back-extracted into ether before being converted through *in situ* diazomethane treatment to the methyl acrylate telomers **10**, which could be readily identified by gas chromatography/mass spectrometry.

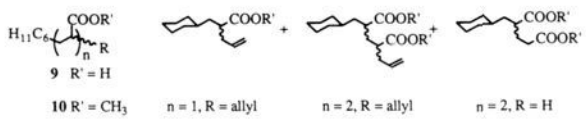

In order to establish retention times for the desired compounds **10** (R = allyl), simple telomerizations of methyl acrylate were conducted using the cyclohexyl iodide/allyltributyltin system. Gas chromatographic analysis furnished the telomer distributions for these reactions, two of which are presented in the form of product histograms in Figure 2. Figure 2a mimics the optimum conditions found for the ACT reaction, substituting methyl acrylate for covalent assembly **4**. The product mixture is composed almost entirely of the first telomer **10** (n = 1, R = allyl). Gradually increasing monomer concentration from 5 mM to 0.5 M resulted in a wider distribution of telomers, as expected. The results for Figure 2b speak to the general limitation of telomerization, namely that of controlling the telomer dispersity. In targeting **10** (n = 2, R = allyl), the yield accomplished through tradiational telomerization is approximately 30%. Moreover, since this represents the sum of all four stereoisomers, the percentage of any specific isomer is only about 8%.

Two ACT conditions were chosen based upon product optimization: 5 mM **4**, 80 mM $C_6H_{11}I$, and 400 mM allyltributyltin (abbreviated as $5^A/80^I/400^{Sn}$ conditions, where the superscripts refer to the assembly, the iodide, and the stannane, respectively) and 2.5 mM **4**, 80 mM $C_6H_{11}I$, and 200 mM allyltributyltin ($2.5^A/80^I/200^{Sn}$ conditions). Reactions were run under each of these conditions and subsequently assayed as described above for product telomer distribution and stereoselectivity. Product histograms for the $5^A/80^I/400^{Sn}$ conditions and the $2.5^A/80^I/200^{Sn}$ conditions are shown in Figure 3a,b.

The success of the ACT strategy is critically dependent upon the ability to balance the rate of chain transfer against the rate of cyclization and the rate of intermolecular addition. If the rate of chain transfer is too high, transfer may precede cyclization, as shown in Scheme 2 to give **6**. With one active monomer remaining, **6** is destined to repeat the addition/transfer cycle and yield the doubly-trapped product. Cyclization could also be prevented by a high rate of intermolecular addition to template **4**. It is clear that cyclization can be promoted by lowering the concentrations of allylstannane and **4**, respectively. In so doing, however, the rate of chain transfer must not drop so low as to allow for extensive intermolecular reaction between the cyclized radical and unreacted assembly **4** or for intramolecular H-atom abstraction.

The results for the reaction run under $5^A/80^I/400^{Sn}$ conditions were promising in some respects (Figure 3a). Comparison to the telomer distribution obtained when methyl acrylate was reacted under identical conditions demonstrates that we have markedly impacted the telomer distribution. The amount of **10** (n = 2, R = allyl or H) obtained from reaction of **4** was about 18 times that from the methyl acrylate case. If the reactions are assumed to be irreversible, then the relative product distribution is indicative of the relative rates of product formation. Furthermore, if intermolecular additions leading to higher telomers are ignored,

(14) For discussions of the mechanism of hydrolysis of oxazolidines, see: (a) Fife, T. H.; Hagopian, L. *J. Am. Chem. Soc.* **1968**, *90*, 1007. (b) Fife, T. H.; Hutchins, J. E. *J. Org. Chem.* **1980**, *45*, 2099. For a leading reference on the mechanism of hydrolysis of amides, see: (c) Brown, R. S.; Bennet, A. J.; Slebocka-Tilk, H. *Acc. Chem. Res.* **1992**, *25*, 481.

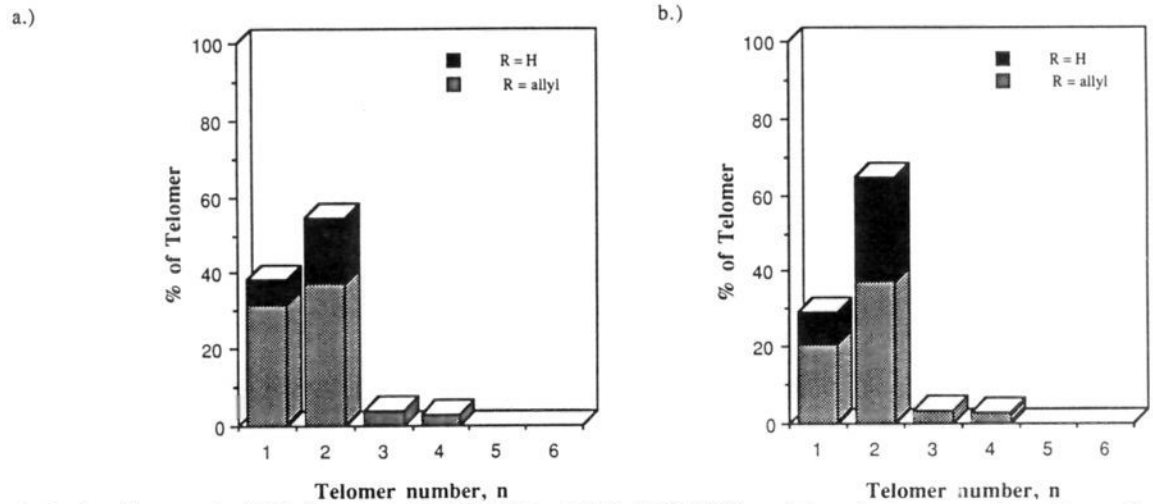

Figure 3. Product histogram for ACT of **4** under (a) $5^{A}/80^{I}/400^{Sn}$ and (b) $2.5^{A}/80^{I}/200^{Sn}$ conditions. Products assayed are telomers **10** with R = H, black and R = allyl, gray.

Scheme 3. Synthesis of Preassembled Tethers[a]

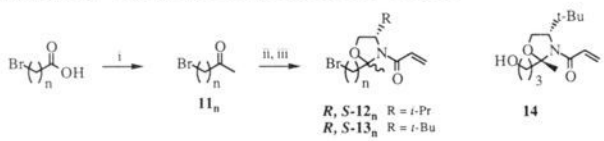

[a] (i) 2 equiv of MeLi, THF, –78 °C; (ii) *S*-valinol or *S*-*tert*-leucinol, CH_2Cl_2, $MgSO_4$; (iii) acryloyl chloride, *N*-methyl morpholine, catalyst DMAP, CH_2Cl_2, 0 °C to room temperature.

it is possible to derive rough estimates for the ratios k_c/k_t (Scheme 2, eq 1). Thus, k_c/k_t can be found from

$$\frac{\mathbf{10}\ (n = 2,\ \mathrm{R} = \mathrm{allyl} + \mathrm{H})}{0.5{\cdot}\mathbf{10}\ (n = 1,\ \mathrm{R} = \mathrm{allyl})} = \frac{\text{rate of cyclization}}{\text{rate of transfer}} = \frac{k_c[\mathbf{5}]}{k_t[\mathbf{5}][\text{stannane}]}\frac{k_c}{k_t} = \frac{\mathbf{10}\ (n = 2,\ \mathrm{R} = \mathrm{allyl} + \mathrm{H})}{0.5{\cdot}\mathbf{10}\ (n = 1,\ \mathrm{R} = \mathrm{allyl})}{\cdot}[\text{stannane}] \quad (1)$$

The amount of **10** (n = 1, R = allyl) is halved since we are assuming that 2 equiv ultimately result from the initial addition and transfer (see Scheme 2). From eq 1, k_c/k_t = {54.94/(0.5)(31.39)}·0.4 M = 1.4 M under $5^{A}/80^{I}/400^{Sn}$ conditions.

H-atom abstractions, along with other intramolecular reactions like cyclization, should be favored over competing intermolecular processes as the reaction mixture is diluted. This proves to be the case, as evidenced by the results shown in Figure 3. For example, the ratio of cyclization/transfer [{**10** (n = 2, R = allyl + H)}/{(0.5)(**10** (n = 1, R = allyl)}] was {54.94/(0.5)(31.39)} = 3.5 under $5^{A}/80^{I}/400^{Sn}$ conditions but rose to {64.62/(0.5)(20.41)} = 6.3 when run at $2.5^{A}/80^{I}/200^{Sn}$. The ratio of H-atom abstraction/transfer [**10** (n = 2, R = H)/**10** (n = 2, R = allyl)] also rose upon dilution, from (17.62/37.32) = 0.47 to (27.27/37.35) = 0.73. These data point to a predominantly intramolecular abstraction process.[15]

Second Generation Templates. Because of the substantial amount of H-atom transfer in the product mixture utilizing template **4**, new templates were sought having structures absent the benzylic hydrogens that are present in this structure. Preassembled oxazolidine acrylamide tethers were generally prepared as indicated in Scheme 3. Thus, slow addition of 2 equiv of methyllithium to commercially available ω-bromo carboxylic acid at –78 °C in THF afforded a 65% yield of the requisite bromoalkyl methyl ketone **11**.[16] The bromoketone was converted through treatment with (*S*)-valinol or (*S*)-*tert*-leucinol as described previously to oxazolidine acrylamides (***R***)- and (***S***)-**12**$_n$ (70–80%) and (***R***)- and (***S***)-**13**$_n$ (65–75%), respectively.

The diastereoisomers for both **12**$_n$ and **13**$_n$ proved to be separable by silica gel flash column chromatography, although removal of trace amounts of unreacted **11**$_n$ from the first eluting diastereomers of **13**$_n$ required normal phase HPLC purification. The assignment of absolute configuration at the quaternary carbon of the oxazolidine was based on nuclear Overhauser enhancement in the ^{1}H NMR and single-crystal X-ray analysis of alcohol **14**. Irradiation of the *tert*-butyl group of first eluting diastereomer ***R*-13**$_n$ generally resulted in a 2.6% enhancement for the signal of the cross-ring methyl group. Similarly, a small enhancement (1.5%) of the *tert*-butyl signal was noted upon irradiation of the methyl substituent. These enhancements were completely absent in the second eluting diastereomer ***S*-13**$_n$.

Attempts to prepare preassembled tethers having three methylene units via reaction of (*S*)-*tert*-leucinol with 5-bromo-2-pentanone failed. Mixing of these two compounds resulted in an exothermic reaction that yielded a cream-colored solid, presumably a hydrobromide salt formed from an intramolecular S_N2 displacement (*5-exo-tet*) of bromide by nitrogen following initial oxazolidine formation. This necessitated a more circuitous route to the halide proceeding through the silyl protected alcohol. The alcohol **14** crystallized from diethyl ether and a single-crystal X-ray analysis was performed to establish unambiguously the suspected *S* absolute configuration of the oxazolidine quaternary carbon. A view of the solid state structure is provided in Figure 4.[17] This alcohol was converted by standard procedures to the corresponding bromide which, consistent with the NOE experiments, proved to be the second eluting compound in silica chromatography. We therefore assign an *R* configuration to the quaternary carbon in all of the first eluting diastereomers and an *S* configuration to the second eluting diastereomers of **13**. Bromides (***R***)-**12**$_n$ and (***S***)-**12**$_n$ were converted to the templates **15**–**17** by reaction of the corresponding aromatic diols in 30% DMSO/acetone with potassium carbonate. The yields of templates were poor (20–30%) when R = H but were 60–80%

(15) We have not identified the source of H-atoms, but positions α to ethers are reactive toward electrophilic or ambiphilic radicals.

(16) (a) Rubottom, G. M.; Kim, C. *J. Org. Chem.* **1983**, *48*, 1550. (b) Jorgenson, M. J. *Org. React.* **1970**, *18*, 1.

(17) The overall oxazolidine geometry in **14** is in excellent accord with that of the corresponding 2,2-dimethyl analog **18**. (Porter, N. A.; Rosenstein, I. J.; Breyer, R. A.; Bruhnke, J. D.; Wu, W.-X.; McPhail, A. T. *J. Am. Chem. Soc.* **1992**, *114*, 7664).

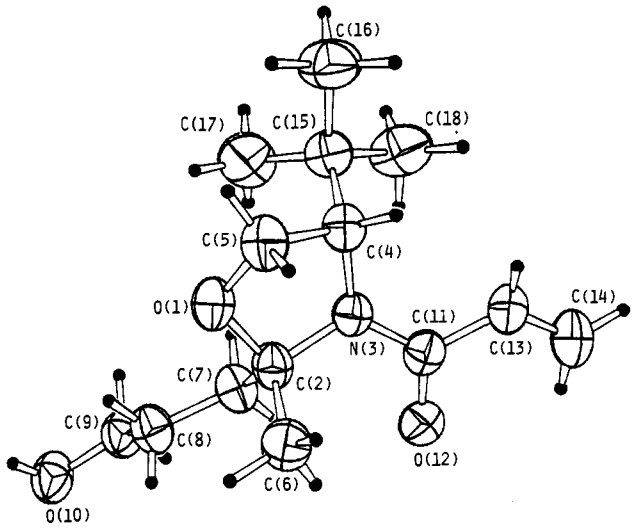

Figure 4. ORTEP diagram (40% probability ellipsoids) showing the atom numbering scheme and solid-state conformation of **14**; small circles represent hydrogen atoms.

when R = COOMe. Some monoalkylation product (<5%) was also generally obtained.

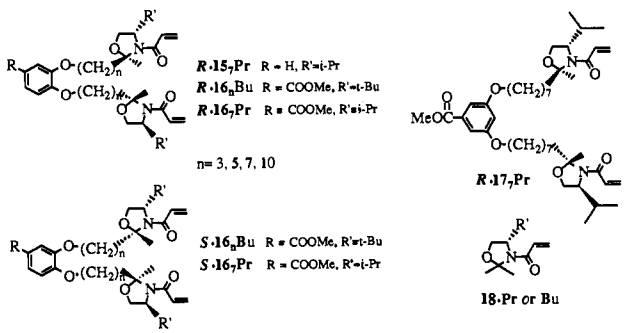

The second generation assembly, (*R*)-**16**$_7$**Pr**, was subjected to the ACT reaction using 2.5 mM template, 80 mM cyclohexyl iodide, and 200 mM allyltri-*n*-butylstannane ($2.5^{A}/80^{I}/200^{Sn}$ conditions) and subsequently assayed to determine its effectiveness. ACT reactions run with templates **15** and **16** were generally indistinguishable, and most studies were carried out on the carbomethoxy compounds because of the better yields of these compounds. The results for (*R*)-**16**$_7$**Pr** shown in Figure 5a represent substantial improvements in several respects over those obtained from assembly **4**. Since the rate of chain transfer should remain relatively constant from template to template, ratios of transfer to abstraction for each intermediate give rasonable estimates of the relative inherent propensity for hydrogen atom abstraction of the two assemblies. Although abstraction remains a significant problem for assembly (*R*)-**16**$_7$**Pr**, products deriving from transannular hydrogen atom abstraction were considerably reduced; the ratio of **10** (n = 2, R = allyl) to **10** (n = 2, R = H) rose sharply from ~1.4 with **4** to 7.2 with (*R*)-**16**$_7$**Pr**. Intramolecular abstraction preceding cyclization was also reduced, but to a lesser extent, with **10** (n = 1, R = allyl) to **10** (n = 1, R = H) ratios climbing to 4.7 from 2.4.

There is a marked dependence of product distribution on template stereochemistry, the *R* templates generally giving more n = 2 products compared to the *S* compounds. This is illustrated in comparison of the product histograms shown in Figure 5a,b. The product histogram for templates (*R*)-**16**$_7$**Bu** is presented in Figure 5c. There is minimal amount of product resulting from H-atom abstraction when **Bu** substrates are examined as compared to **Pr** substrates. We note that templates with R′ = **Bu** are not subject to a potential H-atom transfer from the tertiary isopropyl center of the **Pr** substrates to the α-acrylamido radical.

An ACT reaction was performed on (*R*)-**16**$_7$**Bu** under $2.5^{A}/80^{I}/200^{Sn}$ conditions, and after removal of tin byproducts by standard procedures, a mixture of product macrocycles was isolated in 60% yield by a combination of silica gel flash column chromatography and normal phase HPLC. The chromatographically pure macrocycles gave the expected ^{1}H NMR; integration indicated the presence of one allyl group for each aromatic ring. Several possible isomers were present in the product mixture (regioisomers and stereoisomers), and the spectra (^{1}H and ^{13}C) were complex but consistent with the assigned structures. In a separate ACT reaction of assembly (*R*)-**16**$_7$**Bu** under identical conditions, the methyl acrylate telomers were isolated by flash column chromatography after hydrolysis of the macrocyclic products and methylation. The product mixture was composed of predominantly one n = 2 compound, **10** (R = allyl). The isolated yield for the three step sequence (ACT reaction, hydrolysis and conversion to the methyl esters) was approximately 30%. This yield was adversely affected by detrimental lactonization that occurred upon hydrolysis. We are currently assessing other means of release of the product telomer from the macrocycle to ensure the maximum isolated yield of product. In principle a 60% yield of the telomers **10** (n = 2, R = allyl) could be obtained from a sequence involving ACT and telomer release from macrocycles if a more efficient release reaction could be found.

Construction of the covalent assembly according to the standard alkylation procedure starting with commercially available methyl 3,5-dihydroxybenzoate afforded (*R*)-**17**$_7$**Pr** in 71% yield. An ACT reaction was performed under $2.5^{A}/80^{I}/200^{Sn}$ conditions, and the products were converted to the methyl acrylate telomers via the standard assay protocol. The results of this evaluation, given in Table 1, are of interest in several respects. Based on the assumption that the rate of allyl transfer is comparable for radicals derived from (*R*)-**17**$_7$**Pr** and (*R*)-**16**$_7$**Pr**, we estimate that assembly (**R**)-**17**$_7$**Pr** cyclizes with a rate only (0.49 M/2.8 M) = 0.18 times that of (*R*)-**16**$_7$**Pr**. The intrinsic rate constant for intermolecular addition (k_{inter}) should be the same for both systems, so this represents a 6-fold reduction in the effective molarity upon changing from *ortho*- to *meta*-substitution.

Illuminati and Mandolini have carried out extensive studies on the quantitative aspects of ring-closure reactions.[18,19] In comparing reactivity data for several different series of cyclization reactions, a striking feature emerged in terms of the effective molarities (EM).[19b] EM values converged in the large-ring (ring size ≥ 14) region to a narrow range between 0.1 and 0.01 M. This suggests that the ease of formation of large rings from a bifunctional precursor is substantially independent of the length of the chain, the nature of the functional groups, and the presence of structural moieties other than methylene groups. Baker et al.[20] suggested that structural moieties such as the *o*-phenylene unit should greatly enhance the ease of ring closure of long-chain bifunctional compounds. While the "rigid group effect" is no doubt operative in the medium-ring region, its expression in the formation of very large rings is questionable.[19c] Regardless of how well literature precedent supports this, the fact remains that assemblies constructed from methyl 3,5-dihydroxybenzoate give unacceptable performance in ACT reactions. For this reason, methyl 3,4-dihydroxybenzoate was selected as the exclusive rigid base compound for subsequent studies.

Stereoselectivity. The desired telomer **10** (n = 2, R = allyl) contains two asymmetric centers and thus exists as two diaster-

(18) (a) Illuminati, G.; Mandolini, L. *Acc. Chem. Res.* **1981**, *14*, 95. (b) Kirby, A. J. *Adv. Phys. Org. Chem.* **1980**, *17*, 183.

(19) (a) Dalla Cort, A.; Mandolini, L.; Masci, B. *J. Org. Chem.* **1980**, *45*, 3923. (b) Illuminati, G.; Mandolini, L.; Masci, B. *J. Am. Chem. Soc.* **1977**, *99*, 6308. (c) Mandolini, L.; Masci, B.; Roelens, S. *J. Org. Chem.* **1977**, *42*, 3733. (d) Dalla Cort, A.; Illuminati, G.; Mandolini, L.; Masci, B. *J. Chem. Soc., Perkin Trans. II* **1980**, 1774. For a comprehensive review of the intramolecular reactions of chain molecules, see: (e) Mandolini, L. *Adv. Phys. Org. Chem.* **1986**, *22*, 1.

(20) Baker, W.; McOmie, J. F. W.; Ollis, W. D. *J. Chem. Soc.* **1951**, 200.

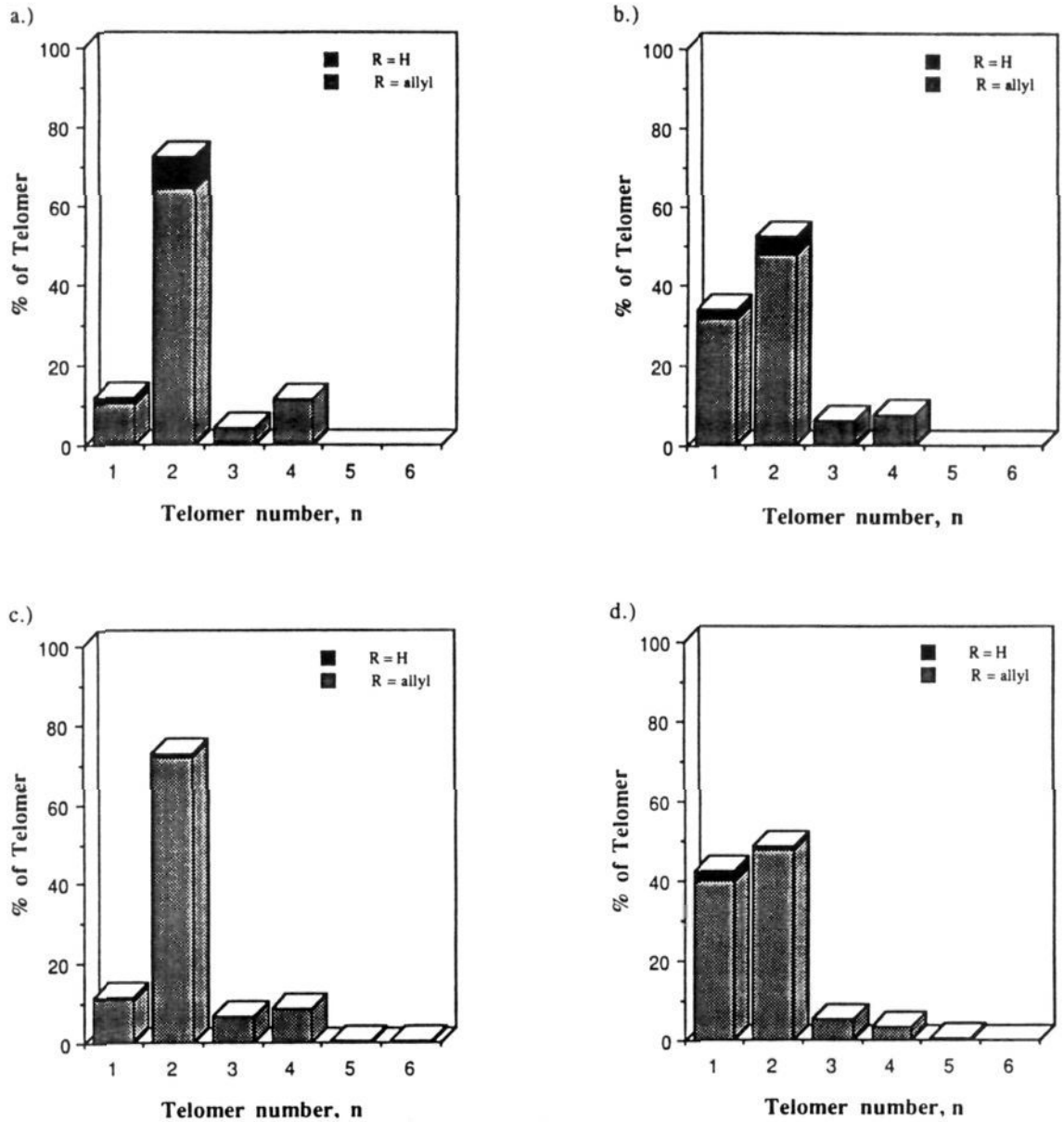

Figure 5. Product histogram for ACT of (***R***)-**16$_7$Pr** under 2.5^A/80^I/200^{Sn} conditions. (b) Product histogram for ACT of (*S*)-**16$_7$Pr** under 2.5^A/80^I/200^{Sn} conditions. (c) Product histogram for ACT of (***R***)-**16$_7$Bu** under 2.5^A/80^I/200^{Sn} conditions. (d) Product histogram for ACT of (***S***)-**17$_7$Pr** under 2.5^A/80^I/200^{Sn} conditions.

eomeric pairs of enantiomers, each giving rise to its own GC signal. Telomerizations of methyl acrylate with cyclohexyl iodide/allyltributyltin showed little stereoselectivity, with a slight preference (1.3:1) for the earlier eluting syndiotactic enantiomeric pair. The ratio of rate constants that determines the selectivity in polymerization of methyl acrylate is $k_{syndiotactic}/k_{isotactic} = 1.1$ at 0 °C.[21] This mild preference for syndiotactic diads has been attributed to the influence of 1,3 allylic strain.

Diastereoselectivity was generally modest (1.5 to 3:1) for **10** ($n = 2$, R = allyl) from the ACT of covalent assemblies bearing the (**Pr**) valinol auxiliary, favoring the later eluting (*isotactic*) pair of enantiomers. The final selectivity, a product of the selectivities for both cyclization and chain transfer, was expected to be moderate for this auxiliary based on reactions of simple acrylamides bearing analogous auxiliaries.[22] Diastereoselectivity was excellent (12 to 23:1) for **10** ($n = 2$, R = allyl) from the ACT of covalent assemblies bearing the (**Bu**) *tert*-leucinol auxiliary, favoring the later eluting (*isotactic*) pair of enantiomers. The anticipated increase in stereoselectivity upon changing from valinol to *tert*-leucinol-derived auxiliaries (based on results for acyclic systems **18Pr** and **18Bu**)[22] was indeed borne out. Diastereoselectivity for **10** ($n = 2$, R = allyl) increased from 3.0:1 (assembly (***R***)-**16$_7$Pr**) to 22:1 (assembly (***R***)-**16$_7$Bu**). The diastereoselectivities in the ACT reactions closely parallel those obtained for the acyclic variants for valinol and *tert*-leucinol derived acrylamides.[22,23]

Subtleties of the selectivity in the ACT reaction are lost when only the ratio of diastereomeric products is considered. Clearly a methodology is needed for the determination of the relative ratios of each of the four individual stereoisomers. We have developed a methodology in which the $n = 2$ diacids are characterized by conversion to the corresponding diastereomeric

(21) For a discussion of factors that influence stereoregulation in the polymerization of vinyl monomers, see: Pino, P.; Sutter, U. W. *Polymer* **1976**, *17*, 977.

(22) Porter, N. A.; Bruhnke, J. D.; Wu, W.-X.; Rosenstein, I. J.; Breyer, R. A. *J. Am. Chem. Soc.* **1991**, *113*, 7788.

(23) Porter, N. A.; Allen, T.; Breyer, R. B. *J. Am. Chem. Soc.* **1992**, *114*, 7676.

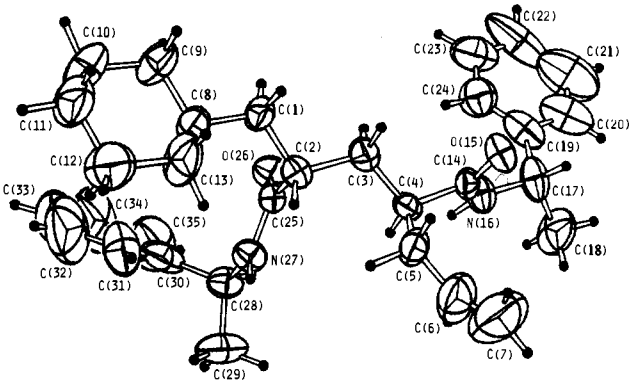

Figure 6. ORTEP diagram (40% probability ellipsoids) showing the atom numbering scheme and solid-state conformation of **19c**; small circles represent hydrogen atoms.

diamides, **19a–d**, with (*S*)-(−)-α-methylbenzylamine. The n = 2 diacids were synthesized independently by (1) Michael addition of the lithium enolate of ethyl cyclohexanepropionate to ethyl 2-methylene-4-pentenoate to give the diethyl esters of the n = 2 telomer and (2) hydrolysis of the diesters in refluxing ethanolic KOH solution. The resulting diacids were converted (oxalyl chloride) to the corresponding diacid chlorides followed by reaction with (*S*)-(−)-α-methylbenzylamine to afford the diastereomeric diamides, **19a–d**. The four diastereomeric diamides are easily separated by GC. Crystals of **19c** (third eluting on GC), the stereoisomer that corresponds to the major diastereomer formed in ACT reactions, were obtained by slow solvent evaporation of a 95% $CHCl_3$:5% EtOAc solution. X-ray crystallographic analysis revealed that the absolute configuration of this isomer is (2*R*,4*S*). A view of the solid state conformation is presented in Figure 6. The high boiling isomer **19d** (derived from the diacid enantiomeric to **9c** (n = 2, R = allyl)) possesses the (2*S*,4*R*) configuration. The absolute configurations of the syndiotactic isomers **9a** and **9b** (n = 2) were established through synthesis of the two diasteeomeric diacids in which the configuration at carbon-2 was controlled. The stereochemical control was achieved in a Michael addition utilizing a carbanion substituted with an oxazolidinone auxiliary derived from (*R*)-(−)-phenylglycinol.[24] Upon conversion of the Michael products to the diamides, **19**, only two peaks were apparent in the appropriate region of the gas chromatogram. Coinjections verified that these peaks corresponded to the first and last eluting isomers, **19a** and **19d**. Since the configuration at C2 is *S*, as expected from the chiral auxiliary, the configuration of **9a** (n = 2) must be (2*S*,4*S*). Thus the second eluting isomer (derived from the enantiomeric diacid) must possess the (2*R*,4*R*) configuration.

There appears to be some small and irreproducible loss of stereochemical configuration in the conversion (hydroxide, oxalyl chloride, phenethylamine) of diesters to **19a–d**. We find that the *isotactic*:*syndiotactic* diasteromer ratio of the diester precursors are not always accurately reproduced in the ratio of diamides formed after hydrolysis and conversion to the diamides. Nevertheless, it is possible to assign the absolute configurations of the major and minor n = 2 telomers from ACT

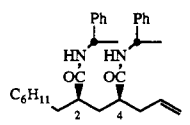

19c

reactions. These results confirm that the absolute configuration of the major and minor ACT products are (2*R*,4*S*) and (2*S*,4*R*), respectively, as expected for auxiliary control. The ratios between the *isotactic* (*i.e. syn, erythro*) and *syndiotactic* (*i.e. anti, threo*) isomers are not quantitative as evidenced by the discrepancy between this ratio for the diamides and initial dimethyl esters. As an example, analysis of n = 2 products from an ACT reaction of (*R*)-**16$_7$Bu** gave a 96:4 *isotactic*:*syndiotactic* diester product ratio and conversion of this diester mixture to diamides **19a–d** gave an **a–d** distribution of 0.06:0.09:0.85:0.0. It is clear from such analyses that the major component of the *isotactic* stereoisomers (**c** and **d**) formed in the ACT reaction are essentially enantiomerically pure and that the *syndiotactic* stereoisomers (**a** and **b**) are nearly racemic, but the *isotactic*:*syndiotactic* product ratio determined from the diamides (85:15) is not within experimental error of the value determined for the precursor diesters (96:4).

Since conditions of the ACT reaction were first examined using the first generation template **4**, an investigation was carried out in which the concentrations of cyclohexyl iodide, allyltributyltin, and covalent assembly (**R**)-**16$_7$Bu** were varied. The results are listed in Table 1. Reduction of template and allylstannane concentrations improves the performance of the ACT reaction, while stereoselectivity is unaffected. Of the conditions examined, reaction at $1^A/80^l/100^{Sn}$ gives the most n = 2 telomer. These conditions, $1^A/80^l/100^{Sn}$, appeared to be a lower limit for the ACT sequence, since at even lower concentrations of template and allylstannane, the chain reaction does not propagate efficiently. At a concentration of 20 mM (*R*)-**16$_7$Bu**, interassembly addition reactions appearently compete with cyclization, since the amount of **10** (n = 4, R = allyl) increased substantially over the reaction run at 5 mM concentration, from 6.41% to an average value of 18.9%. The proportion of this telomer does not increase significantly upon increasing the concentration of (*R*)-**16$_7$Bu** to 50 mM. Since there were likely telomers **10** ($n \geq 7$) in the product mixture of this last reaction, and these cannot be detected in the assay, the relative percentages reported for telomers **10** (n = 1–6) are probably higher than the actual percentages. The maximum attainable percentage of **10** (n = 4, R = allyl) by this approach appears to be about 20%.

Trends in Performance Characteristics for Second Generation Covalent Assemblies. With regard to cyclization efficiency for a given tether length, the assembly prepared from (*R*)-**12$_n$** and (*R*)-**13$_n$** tethers (n = 3, 5, 7, 10) consistently outperformed the diastereomeric counterpart constructed from the (*S*)-**12$_n$** and (*S*)-**13$_n$** tethers. It appears that cyclization efficiency (which can be estimated by the ratio k_c/k_t) exhibits a universal stereochemical dependence. Moreover, the dependence is more pronounced when valinol-derived auxiliaries are used than for the leucinol compounds.

Given the complexity of the systems, the exact origin of this phenomenon is uncertain, but one possible explanation is presented in Figure 7.[17] Consider the preferred *Z* N–C(O) rotamers of the acyclic intermediate radicals illustrated at the left of the figure. For (*R*)-**12$_n$** and (*R*)-**13$_n$** tethers, the blocking group and the remainder of the assembly are *trans* to one another across the oxazolidine ring. This arrangement places the reactive acrylamide monomer on the open face of the prochiral radical center and therefore favors cyclization. The blocking group and the remainder of the assembly are *cis* to one another, however, for (*S*)-**12$_n$** and (*S*)-**13$_n$** tethers, a configuration that impedes cyclization by positioning the pendant olefin on the closed face of the prochiral radical.

The cyclization efficiency is dependent not only on the tether configuration but also on the length of the tether. The cyclization efficiency, expressed as the value of k_c/k_t, is plotted against the number of tether methylene units in Figure 8.

The arguments offered to explain stereochemical dependence would predict that the difference in cyclization efficiencies between diastereomeric assemblies should increase as tether length decreases, since for extremely long tethers, increased confor-

(24) Evans, D. A.; Bilodeau, M. T.; Clardy, J.; Cherry, D.; Kato, Y. *J. Org. Chem.* **1991**, *56*, 5750.

Table 1. Diastereoselectivities and Relative % of Telomers **10** from ACT Reactions of Covalent Assemblies[a]

		10 (R = H)		**10** (R = allyl)[b]					
assembly	D^c	$n = 1$	$n = 2$	$n = 1$	$n = 2$	$n = 3$	$n = 4$	$n = 5$	$n = 6$
(*S*)-16_7Bu[d]	18.2	0.3_0	0.6_3	18.0_0	63.0_4	6.6_2	10.0_7	0.5_8	0.7_8
(*R*)-16_7Bu[e]	22.9	0.4_6	1.6_6	6.4_7	78.8_9	5.7_7	6.7_5	0.0_0	0.0_0
(*R*)-16_7Bu[d]	21.8	0.5_2	0.6_8	10.8_9	72.0_3	6.4_6	8.7_7	0.2_5	0.3_9
(*R*)-16_7Bu[f]	22.7	0.3_8	0.7_1	17.4_7	66.7_0	7.7_8	6.4_1	0.3_0	0.2_2
(*R*)-16_7Bu[g]	21.4	0.5_2	1.0_4	12.4_2	47.0_9	14.2_6	17.9_9	2.5_5	4.1_3
(*R*)-16_7Bu[h]	17.9	0.6_6	1.4_3	10.4_8	29.8_5	16.8_9	20.2_7	9.6_2	10.8_0

[a] Based on GC integration; average of triplicate analysis. [b] Includes lactonized telomers. [c] Diastereoselectivity; based on ratio of GC integrated areas of major and minor diastereomeric **10** ($n = 2$, R = allyl) pairs. [d] $2.5^{A}/80^{I}/200^{Sn}$. [e] $1^{A}/80^{I}/100^{Sn}$. [f] $5^{A}/80^{I}/200^{Sn}$. [g] $20^{A}/80^{I}/200^{Sn}$. [h] $50^{A}/80^{I}/200^{Sn}$.

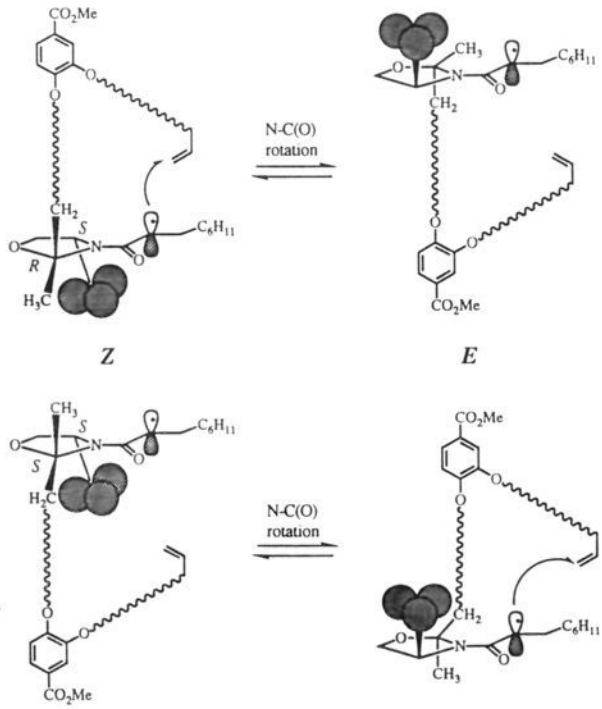

Figure 7. Possible explanation for the dependence of cyclization efficiency on oxazolidine configuration and auxiliary blocking group.

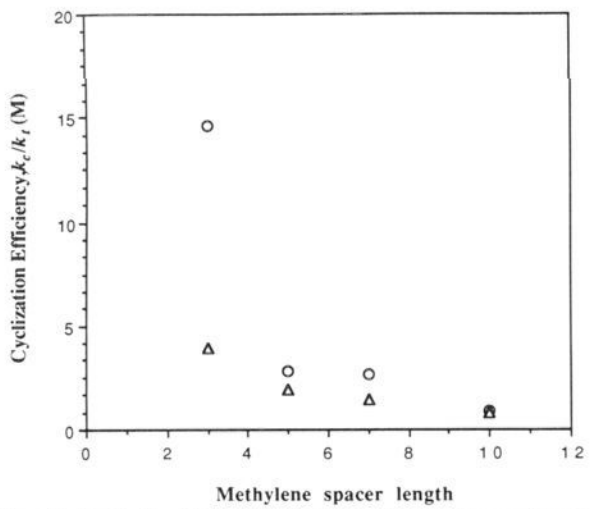

Figure 8. Cyclization efficiency for diastereomeric assemblies as a function of the number of methylene units in the tether. Circles are for (***R***)-**16$_n$Bu**, and triangles are for (***S***)-**16$_n$Bu** where n is the methylene spacer length.

mational flexibility negates the importance of the tether configuration. Generally this proved to be the case. Cyclization of (***R***)-**16$_{10}$Bu** or (***S***)-**16$_{10}$Bu** to a 33-membered ring was virtually insensitive to tether configuration, while for the shortest tether,

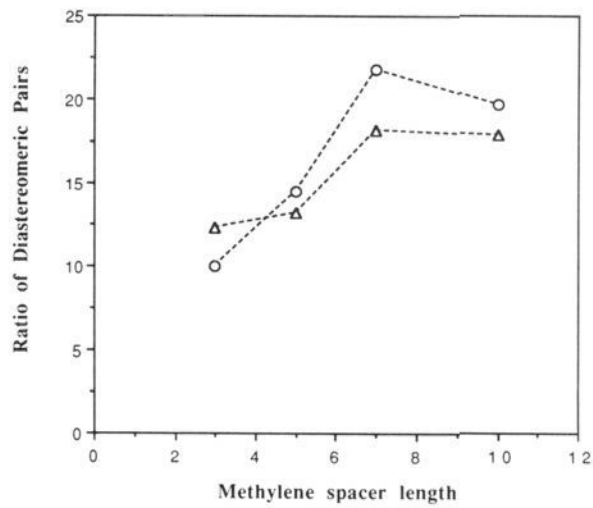

Figure 9. Diastereoselectivity for **10** ($n = 2$, R = allyl) for diastereomeric assemblies as a function of the number of methylene units in the tether. Circles are for (***R***)-**16$_n$Bu**, and triangles are for (***S***)-**16$_n$Bu** where n is the methylene spacer length.

a marked difference was observed in formation of the 19-membered ring.

Were the objective preparation of **10** ($n = 2$, R = allyl) without regard to stereochemistry, covalent assembly (***R***)-**16$_3$Bu** would be best suited. This investigation, however, targets a particular stereoisomer, and the dependence of stereoselectivity on tether length and oxazolidine configuration must be considered. The diastereoselectivity for **10** ($n = 2$, R = allyl) is plotted against the number of tether methylene units in Figure 9.

Assuming that cyclization occurs with similar selectivity for all assemblies, the differences exhibited above are due to variations in the stereoselectivity of chain transfer. For large ring sizes, the cyclic intermediate radical can be treated as if it were acyclic, and the stereoselectivity should approach that observed in model acyclic systems. The measured diastereoselectivity for assemblies forming 27- and 33-membered rings (roughly 20:1) is similar to that observed when **18-Bu** undergoes the analogous addition-transfer sequence (25:1).[22] In this region, assemblies prepared from (***R***)-**12$_n$** and (***R***)-**13$_n$** tethers show slightly higher diastereoselectivity than those constructed from the corresponding *S* diasteromer.

The diastereoselectivity decreases as the ring size drops below 27. Transannular strain is minimal in unsubstituted cycloalkanes with ring sizes greater than 15. For highly substituted cycloalkanes, however, substantial transannular strain might exist in 19- and even 23-membered rings. Developing transannular strain may account for the decrease in stereoselectivity as ring size is decreased. For reasons not understood, assemblies constructed from (***R***)-**13$_n$** tethers are more sensitive to ring-size effects (22:1 to 10:1) than those prepared from (***S***)-**13$_n$** tethers (18:1 to 12:1).

The trends in cyclization and diastereoselectivity are opposite and will tend to offset each other to a certain degree. A measure of the trade-off between these desirable traits can be gained by

Table 2. Cyclization Efficiencies, Diastereoselectivities, and Efficiency Factors for Diastereomeric *tert*-Leucinol-Derived Covalent Assemblies of Different Tether Length[a]

assembly	cyclization eff,[b] M	diastereoselectivity[c]	EF,[d] %
(*R*)-16$_3$Bu	14.6	10.0	79.3
(*R*)-16$_5$Bu	2.80	14.5	75.3
(*R*)-16$_7$Bu	2.67	21.8	68.9
(*R*)-16$_{10}$Bu	0.90	19.7	59.9
(*S*)-16$_3$Bu	3.96	12.3	62.8
(*S*)-16$_5$Bu	1.96	13.2	71.4
(*S*)-16$_7$Bu	1.41	18.2	59.8
(*S*)-16$_{10}$Bu	0.78	17.9	53.6

[a] Conditions: 2.5^A/80^I/200^{Sn}. [b] Calculated from eq 1. [c] Determined from GC integrated areas of major and minor diastereomeric pairs of **10** (n = 2, R = allyl). [d] Calculated from eq 2.

calculating an efficiency factor (EF), as shown in eq 2. The cyclization efficiencies (as measured by k_c/k_t values), diastereoselectivities, and efficiency factors for assemblies of interest are collected in Table 2.

$$\mathrm{EF} = \left[\frac{\{\mathbf{10}\ (n = 2, \mathrm{R} = \mathrm{allyl})_{\mathrm{major}}\}\cdot\{\%\ \mathrm{of}\ \mathbf{10}\ (n = 2, \mathrm{R} = \mathrm{allyl})\}}{\mathbf{10}\ (n = 2, \mathrm{R} = \mathrm{allyl})_{\mathrm{major}} + \mathbf{10}\ (n = 2, \mathrm{R} = \mathrm{allyl})_{\mathrm{minor}}}\right] \quad (2)$$

This analysis makes it clear that the loss in diastereoselectivity suffered as tether length decreases is more than offset by the increased efficiency of cyclization, at least for assemblies constructed with ***R*** tethers. The diastereomeric counterparts follow the same general trend, except that an unexplained propensity for the **(*S*)-16$_3$Bu** to participate in intertemplate reactions allowed **(*S*)-16$_5$Bu** to attain the best EF within this series.

Extensions and Prospects. While preparation of diastereomerically pure covalent assemblies proved exceedingly useful in revealing stereochemical intricacies of the ACT reaction, it is untenable from a practical standpoint. ACT reactions run on mixtures of diastereomeric assemblies may lead to somewhat lower performance, but this will be offset by the economic use of the chiral auxiliary and the elimination of excessive chromatography. Based upon the results obtained for diastereomerically pure assemblies, diastereomeric mixtures with one of three different tether lengths (1, 3, or 5) were evaluated for overall performance. These mixtures can be prepared from a bis-ketone template, a procedure that is compatible with the goal of recycling the template. Note that the diastereomeric mixture of templates is not a simple mixture of **(*R*)-16$_n$Bu** and **(*S*)-16$_n$Bu** but contains mixed systems where one tether has the *R* configuration at the oxazolidine quaternary carbon and the other has the *S* configuration at this center. Studies indicate that formation of a 23-membered ring (corresponding to five methylene units in each tether) gives the best results in such systems; the performance matches that of the better of the two pure diastereomers, **(*R*)-16$_5$Bu**.

This work establishes the ACT strategy as a viable means for the preparation of compounds containing isotactic 1,3-stereocenters. It proved possible not only to demonstrate the feasibility of the strategy but also to refine it significantly through systematic variation of the components of the covalent assembly. All components of the system were examined: the rigid base compound, the functionality linking the base compound to the tethers, the length of the tethers, the configuration at the site of oxazolidine attachment, and the auxiliary blocking group. Each of these variables was found to have a profound influence on the performance of the covalent assembly.

Further refinements to the strategy are inevitable and necessary. Having identified the combination of components that give the best overall performance, questions of practicality that remain are currently being addressed, and extension of the methodology both to higher telomers with 1,3-stereocenters and to the preparation of 1,5-stereocenters will be reported in due course.

Experimental Section

General Procedures. Tetrahydrofuran was freshly distilled from sodium benzophenone. Benzene was distilled from sodium onto molecular sieves. Dichloromethane was distilled from calcium hydride onto molecular sieves. Triethylamine, diisopropylamine, diisopropylethylamine, and pyridine were distilled from calcium hydride onto potassium hydroxide. Reactions were run under argon unless otherwise noted. Gas chromatography was performed on a Hewlett-Packard 5890A or 5890II gas chromatograph with a flame ionization detector coupled to a Hewlett-Packard 3393A integrator (conditions, unless otherwise stated: 15 m, 0.32 mm i.d. SPB-1 column; 5 psi; 1 min at 100–280 °C at 15 °C/min). ^{1}H and ^{13}C NMR spectra were recorded on either a Varian XL-300 or a General Electric QE-300 spectrometer with Me_4Si as an internal standard in $CDCl_3$. IR spectra were recorded on a Bomem Michelson Series BM-100 FTIR spectrophotometer. Mass spectra were obtained on a Hewlett-Packard 5988A gas chromatograph/VG-ZAB 1F mass spectrometer. Methane/ammonia (2×10^{-4} atm) was employed for chemical ionization MS. Melting points were taken on a Thomas-Hoover capillary melting point apparatus and are uncorrected. Elemental analysis was performed by Atlantic Microlabs (Atlanta, GA).

Thin layer chromatography was performed using 0.2 mm layer thickness silica gel coated aluminum (60 F_{254}, EM), and TLC plates were visualized by UV_{254}, iodine, or ceric ammonium nitrate, bromocresol green, or phosphomolybdic acid char. Flash column chromatography was carried out using 35–70 μm silica gel. A Waters M6000 or ISCO Model 2350 pump with either a Waters R401 differential refractometer or Waters 441 Absorbance detector (254 nm) was used for HPLC. Preparative HPLC used a Dynamax 60A Si 83-121-C5 silica column (normal phase) or a Dynamax C-18 column (reverse phase). Analytical HPLC used tandem Beckman Ultrasphere Si-4.6 mm × 25 cm columns (normal phase) or tandem Beckman ODS 4.6 mm × 25 cm (reverse phase) columns. HPLC solvents were filtered through Rainin Nylon 66 (0.45 μm pore size) filters. Unless otherwise specified, reagents were used as supplied from Aldrich Chemical Company. Acryloyl chloride was freshly distilled before use. To avoid polymerization, covalent assemblies were generally stored as dilute solutions in benzene at 0 °C.

First Generation Covalent Assemblies. 1,2-Bis(3-methyl-3-((butenyloxy)methyl)benzene, 20. A round-bottom flask was charged with 1.054 g (26.34 mmol, 2.52 equiv) of NaH (60% dispersion in oil). The NaH was washed with 3 × 4 mL *n*-pentane and slurried in 50 mL of THF. Over the course of 5 min, 2.42 mL (2.064 g, 23.97 mmol, 2.29 equiv) of 3-methyl-3-butene-1-ol was added to the slurry at room temperature. The resulting mixture was refluxed for 40 min before being charged dropwise with a solution of 2.759 g (10.45 mmol, 1.0 equiv) of 1,2-bis(bromomethyl)-benzene and 201.5 mg (0.546 mmol, 0.05 equiv) of Bu_4NI in 10 mL of THF. The mixture was refluxed 9 h, then cooled to room temperature, diluted with 50 mL of ether, and washed with 1 × 100 mL saturated NH_4Cl. The organic layer was diluted further with 100 mL of ether, washed with 1 × 100 mL saturated NaCl, dried over $MgSO_4$, filtered, and condensed to a bronze oil that was purified by flash column chromatography (5% EtOAc/hexane), giving 1.690 g (6.16 mmol, 59%) of a clear orange oil: TLC (5% EtOAc/hexane) R_f 0.18, GC (1 min at 100–300 °C at 15 °C/min) t_R 7.99 min; GC/CIMS (CH_4/NH_3(g)) m/z 275 (MH^+), 292 ($M + NH_4$)$^+$; ^{1}H NMR (300 MHz, $CDCl_3$) δ 7.43–7.25 (m, 4H), 4.77 (d, J = 13.2 Hz, 4 H), 4.59 (s, 4H), 3.59 (t, J = 6.9 Hz, 4H), 2.34 (t, J = 6.8 Hz, 4H), 1.75 (s, 6H) ppm; ^{13}C NMR (75 MHz, $CDCl_3$) δ 142.86, 136.51, 128.54, 127.63, 111.48, 70.45, 68.81, 37.83, 22.70 ppm. FTIR (neat, NaCl) 3074, 2967, 2936, 2861, 1650, 1450, 1373, 1359, 1124, 1097, 888, 753 cm^{-1}. Anal. Calcd for $C_{18}H_{26}O_2$: C, 78.79; H, 9.55. Found: C, 78.84; H, 9.47.

1,2-Bis(3-((oxobutyloxy)methyl)benzene, 3, Scheme 1. A solution of 272.4 mg (0.993 mmol) of **20** in 10.0 mL of CH_2Cl_2:MeOH (4:1) was cooled to −78 °C and treated with ozone until the solution maintained a light blue color. Excess ozone was quenched by addition of 1.0 mL of dimethyl sulfide. Solvent was removed under vacuum, and the oil was

(25) See paragraph at the end of the paper regarding supplementary material.

(26) *International Tables for X-ray Crystallography*; Kynoch: Birmingham, U. K., 1974; Vol. IV.

purified by flash column chromatography (60% EtOAc/hexane) to give 227.0 mg (0.816 mmol, 82%) of **3** as a clear yellow oil: TLC (60% EtOAc/hexane) R_f 0.22, GC t_R 9.13 min; ^{1}H NMR (300 MHz, $CDCl_3$) δ 7.38–7.32 (m, 2H), 7.30–7.24 (m, 2H), 4.57 (s, 4H), 3.76 (t, J = 6.2 Hz, 4H), 2.74 (t, J = 6.2 Hz, 4H), 2.19 (s, 6H) ppm; ^{13}C NMR (75 MHz, $CDCl_3$) δ 206.94, 136.10, 128.61, 127.70, 70.59, 65.22, 43.54, 30.32 ppm; FTIR (neat, NaCl) 3066, 3000, 2885, 1714, 1454, 1421, 1364, 1229, 1175, 1123, 1093, 1046, 1004, 951, 757 cm^{-1}. Anal. Calcd for $C_{16}H_{22}O_4$: C, 69.04; H, 7.97. Found: C, 68.90; H, 8.02.

Covalent Assembly 4. A mixture of 3.342 g (12.01 mmol) of **3** and 3.72 g (36.1 mmol, 3.0 equiv) of (*S*)-(+)-2-amino-3-methylbutanol was stirred neat under Ar at room temperature for 1.5 h. The mixture was charged with 64.2 mL of CH_2Cl_2 and some 4Å molecular sieves and stirred overnight. The sieves were removed by filtration, and the filtrate condensed to a light yellow oil that was dissolved in 100 mL of xylenes, washed with 4 × 25 mL saturated $NaHCO_3$ and 1 × 25 mL saturated NaCl solution, and dried over Na_2SO_4. The drying agent was removed by filtration, and the filtrate condensed under vacuum. The residual oil was dissolved in 64.2 mL of fresh CH_2Cl_2, charged with 73.5 mg (0.602 mmol, 0.05 equiv) of DMAP and 3.05 mL (2.81 g, 27.7 mmol, 2.31 equiv) of 4-methylmorpholine, and cooled to 0 °C. To this solution was added dropwise over the course of 25 min 2.15 mL (2.40 g, 26.5 mmol, 2.20 equiv) of acryloyl chloride, and the mixture was warmed to room temperature overnight. The reaction mixture was condensed, dissolved in 100 mL of ether, and filtered. The filtrate, diluted with an additional 200 mL of ether, was washed with 1 × 50 mL saturated $NaHCO_3$, 1 × 50 mL saturated NaCl solution and dried over $MgSO_4$. The drying agent was removed, and the filtrate condensed to a light yellow oil that was further purified by flash column chromatography (75% EtOAc/hexane) and preparative normal phase HPLC (70% EtOAc/hexane) to yield 3.713 g (6.67 mmol, 55%) of assembly **4** as a 1:3.7:3.0 mixture of diastereoisomers. The assembly was stored at 0 °C as a 9.25 mM solution in benzene: TLC (75% EtOAc/hexane) R_f 0.34, GC (1 min at 100–300 °C at 15 °C/min) t_R 20.44, 20.80, and 21.15 min; GC/CIMS (CH_4/NH_3(g)) m/z 557 (MH^+) for each diastereomer; ^{1}H NMR (300 MHz, $CDCl_3$) δ 7.42–7.20 (m, 4H), 6.44–6.34 (m, 4H), 5.70–5.64 (m, 2H), 4.60–4.48 (m, 4H), 4.0–3.5 (m, 10H), 2.86–1.90 (series of m, 6H), 1.70 and 1.57 (s, ratio of 1:2, total 6H), 0.96–0.90 (m, 12H) ppm; ^{13}C NMR (75 MHz, $CDCl_3$) δ 163.25, 162.99, 136.37, 136.30, 136.25, 129.76, 129.66, 128.35, 128.25, 128.16, 127.76, 127.41, 96.25, 70.24, 66.44, 66.34, 65.12, 64.82, 62.03, 61.96, 38.48, 35.09, 31.88, 24.41, 21.02, 19.76, 19.66, 17.89, 16.93 ppm; FTIR (neat, NaCl) 2959, 2875, 1649, 1610, 1466, 1420, 1364, 1295, 1235, 1180, 1125, 1091, 1071, 980, 858, 796, 756 cm^{-1}. Anal. Calcd for $C_{32}H_{48}N_2O_6$: C, 69.04; H, 8.69; N, 5.03. Found: C, 68.93; H, 8.68; N, 4.98.

General Procedure for Additional/Cyclization/Transfer under Standard Conditions. Approximately 0.1435 mmol of the desired template, delivered from a benzene stock solution, is added to 594 μL (0.965 g, 4.59 mmol, 32.0 equiv) of cyclohexyl iodide and 3.56 mL (3.802 g, 11.48 mmol, 80.0 equiv) of allylstannane. The mixture is diluted with benzene to a total volume of 57.4 mL and subsequently purged at room temperature with Ar for 30 min. After purging, 4.7 mg (0.028 mmol, 0.2 equiv) of AIBN is charged into the reaction, and the flask is immersed in an 85 °C oil bath to establish a gentle reflux. A second portion of AIBN is added after 2 h, and reflux is maintained for 10 h. The mixture is cooled to room temperature, and the solvent was removed under reduced pressure. The residual oil is subjected to flash column chromatography using gradient elution (100% hexane → 5%, 10%, 15%, 25%, 50%, 75% EtOAc → 100% EtOAc), and the isolated products are dissolved in Et_2O and stirred overnight over an aqueous 10% KF solution. The layers are separated, and the organic layer dried over $MgSO_4$, condensed, dissolved in EtOAc, refiltered, and condensed to an oil.

General Telomer Assay Procedure. The isolated oil is mixed with 3 mL of 4 N HCl and 3 mL of *p*-dioxane and refluxed for 12 h. The reaction mixture is poured into 100 mL of 1 M KOH and washed 1 × 50 mL of Et_2O. The aqueous layer is cooled to 0 °C, acidified with 10 mL concentrated HCl, and then stirred for 1 h with 50 mL of Et_2O while saturating the aqueous layer with NaCl. The layers are separated, and the aqueous further extracted 2 × 50 mL of Et_2O. The pooled ethereal extracts are dried over $MgSO_4$, filtered, condensed at room temperature to a total volume of about 5 mL, and treated at 0 °C with an excess of diazomethane generated from 0.5–1.0 g Diazald. After warming to room temperature and standing 30 min, excess diazomethane is quenched with a minimum amount of glacial acetic acid. The solution is washed with 1 × 25 mL saturated $NaHCO_3$, dried over $MgSO_4$, and filtered. The filtrate is analyzed by GC (15m SPB-1, 0.32 mm I.D., 5 psi; 1 min at 80 °C, ramp 15 °C/min to 300 °C and hold for 5 min; calibrated vs an authentic mixture of methyl acrylate telomers), and assignments are confirmed by GC/MS. Approximate retention times for telomers of interest are given in Table 3.

Table 3. Approximate GC Retention Times (min) for Telomers **10**

n	R = H	R = allyl	n	R = H	R = allyl
1	3.98	5.54	4		14.03
2	8.05	9.01			14.11
		9.18	5		15.92
3		11.77			15.98
		11.82	6		18.27
		11.87			18.35
		11.92			

Second Generation Covalent Assemblies. The Procedure is Described for Preparation of (*R*)- and (*S*)-16$_7$Bu and Is Illustrative. 9-Bromononan-2-one, 11$_7$. 8-Bromooctanoic (8.97 g, 40.2 mmol) acid was dissolved in THF (270 mL). The reaction was cooled to −78 °C, and a 1.4 M solution of CH_3Li (57.5 mL, 80.4 mmol) in diethyl ether was added dropwise over 20 min. The reaction mixture was allowed to warm to 0 °C over the course of 1 h and quenched with saturated NH_4Cl aqueous solution followed by extraction with diethyl ether. The ether phase was separated, dried over $MgSO_4$, and concentrated. Purification by silica gel flash column chromatography (85:15 hexane:ethyl acetate) gave 5.6 g (63%) of a colorless oil: TLC R_f 0.4 (75:25 hexane:ethyl acetate); ^{1}H NMR (300 MHz, $CDCl_3$) δ 3.34 (t, J = 6.81 Hz, 2H), 2.37 (t, J = 7.38 Hz, 2H), 2.08 (s, 3H), 1.8–1.7 (m, 2H), 1.5 (m, 2H), 1.4–1.2 (m, 6H); ^{13}C NMR (75 MHz, $CDCl_3$) δ 208.6, 43.3, 33.7, 32.4, 29.6, 28.6, 28.2, 27.6, 23.3; FTIR (neat) 2931, 2856, 1714, 1360 cm^{-1}; MS (GC/CIMS) m/z 238(M + NH_4^+); Anal. Calcd. for C9H17BrO: C, 48.88; H, 7.76; found: C, 48.95; H, 7.72.

***(2R,4S)*- and *(2S,4S)*-2-(7-Bromoheptyl)-2-methyl-3-acryloyl-4-*tert*-butyloxazolidine (*R*)- and (*S*)-13$_7$.** A mixture of 66.3 mg (0.300 mmol, 1.0 equiv) of **11$_7$** and 220 mg (1.88 mmol, 6.3 equiv) of 2*S*-amino-3,3-dimethyl-1-butanol was stirred neat for 1 h, after which 243 mg of anhydrous $MgSO_4$, 10.0 mg of *p*-TsOH, and 2.4 mL of CH_2Cl_2 were charged into the flask. The heterogeneous mixture was stirred overnight, and the $MgSO_4$ was removed by filtration. The filtrate was diluted with 15 mL of CH_2Cl_2, washed with 2 × 10 mL saturated $NaHCO_3$, dried over Na_2SO_4, filtered, and condensed to give 81.7 mg of oil. The oil was dissolved in 2.5 mL of CH_2Cl_2, charged with 5 mg of DMAP, and cooled to 0 °C. The solution was charged with 61.7 μL of 4-methylmorpholine and, dropwise over the course of about 1 min, 41.4 μL of acryloyl chloride. The reaction was maintained at 0 °C for 0.5 h, warmed to room temperature overnight, diluted with 10 mL of CH_2Cl_2, washed with 3 × 10 mL saturated $NaHCO_3$, dried over Na_2SO_4, filtered, and condensed to a dark yellow oil that was purified by flash column chromatography (15% EtOAc/hexane) to afford 75.1 mg (0.201 mmol, 67%) of a mixture of (*R*)-13$_7$ and (*S*)-13$_7$.

First eluting (2*R*,4*S*) diastereomer *R*-13$_7$: TLC (15% EtOAc/hexane) R_f 0.29, GC (195 °C, isothermal) t_R 9.81 min; GC/CIMS (CH_4/NH_3-(g)) m/z 376, 374 (MH^+); ^{1}H NMR (300 MHz, $CDCl_3$) δ 6.47 (d of d, J = 16.7, 10.1 Hz, 1H; CH_2=CHR), 6.26 (d of d, J = 16.7, 1.5 Hz, 1H; HCH=CHR), 5.62–5.52 (m, 1H; HCH=CHR: 60 °C; δ 5.56, d of d, J = 10.1, 1.5 Hz, 1H), 4.35 (br d, 6.3 Hz, 1H; NCH, minor rotational isomer), 3.98–3.77 (m, 2H; OCH_2), 3.77–3.66 (m, 1H; NCH, major rotational isomer), 3.31 (t, J = 6.8 Hz, 2H; $BrCH_2$), 2.32–2.18 (m, 1H; diastereotopic HCHC(O)(N)CH_3, major), 1.75 (quintet, J = 7.0 Hz, 2H; $BrCH_2CH_2$), 1.70 (s, 3H; RC(O)(N)CH_3), 1.60–1.45 (m, 1H; diastereotopic HCHC(O)(N)CH_3, major), 1.4–1.1 (m, 8H; $Br(CH_2)_2$-$(CH_2)_4$), 0.875 (s, 9H; *tert*-Bu, major), 0.842 (s, 9H; *tert*-Bu, minor) ppm. ^{13}C NMR (75 MHz, $CDCl_3$) δ 166.02 (C=O, minor rotational isomer), 164.66 (C=O, major rotational isomer), 130.62 (CH_2=CHR, major), 129.57 (CH_2=CHR, minor), 127.24 (CH_2=CHR, minor), 127.01 (CH_2=CHR, major), 98.16 (RC(O)(N)CH_3, major), 95.83 (RC(O)(N)CH_3, minor), 65.17 (OCH_2, major), 64.58 (NCH, major), 64.00 (OCH_2 and NCH, minor), 39.47, 35.78 ($C(CH_3)_3$, minor), 35.71 ($C(CH_3)_3$, major), 34.62 ($CH_2C(O)(N)CH_3$), 33.85 ($BrCH_2$, major), 33.76 ($BrCH_2$, minor), 32.59 ($BrCH_2CH_2$, major), 32.52 ($BrCH_2CH_2$, minor), 29.38 (CH_2, major), 29.23 (CH_2, minor), 28.50 (CH_2, major), 28.41 (CH_2, minor), 27.87 (CH_2, major), 27.78 (CH_2, minor), 27.53 and 27.48 ($C(CH_3)_3$, major), 27.20 and 27.15 ($C(CH_3)_3$, minor), 25.67 (RC-(O)(N)CH_3, minor), 24.08 (CH_2), 23.85 (RC(O)(N)CH_3, major); FTIR (film) 2940, 2865, 1650, 1610, 1415 cm^{-1}. Anal. Calcd for $C_{18}H_{32}$-$BrNO_2$: C, 57.75; H, 8.62; N, 3.74. Found: C, 57.84; H, 8.61; N, 3.75.

Second eluting (2*S*,4*S*)diastereomer *S*-13$_7$: TLC R_f 0.19 (15% EtOAc/hexane); GC t_R 9.60 min (195 °C, isothermal); ^{1}H NMR (300 MHz, $CDCl_3$) δ 6.46 (d of d, J = 16.6, 10.1 Hz, 1H; CH_2=CHR), 6.25 (d of d, J = 16.6, 2.1 Hz, 1H; HCH=CHR), 5.62–5.5 (m, 1H; HCH=CHR: 60 °C; δ 5.54, d of d, J = 10.2, 2.1 Hz, 1H), 4.32 (br d, J = 5.0 Hz, 1H; NCH, minor rotational isomer), 3.98–3.77 (m, 2H; OCH_2), 3.75–3.65 (m, 1H; NCH, major rotational isomer), 3.30 (t, J = 6.8 Hz, 2H; $BrCH_2$), 2.56–2.4 (m, 1H; diastereotopic HCHC(O)(N)CH_3, major), 1.75 (quintet, J = 7.1 Hz, 2H; $BrCH_2CH_2$), 1.70–1.57 (m, 1H; diastereotopic HCHC-(O)(N)CH_3, major), 1.42 (s, 3H; RC(O)(N)CH_3), 1.5–1.1 (m, 8H; Br-$(CH_2)_2(CH_2)_4$), 0.86 (s, 9H; *tert*-Bu,) ppm. ^{13}C NMR (75 MHz, $CDCl_3$) δ 166.13 (C=O, minor rotational isomer), 164.75 (C=O, major rotational isomer), 130.60 (CH_2=CHR, major), 129.58 (CH_2=CHR, minor), 127.30 (CH_2=CHR, minor), 126.95 (CH_2=CHR, major), 97.96 (RC(O)(N)CH_3, major), 95.62 (RC(O)(N)CH_3, minor), 64.88 (OCH_2, major), 64.41 (NCH, major), 63.84 (NCH, minor), 63.67 (OCH_2, minor), 41.04 (CH_2, minor), 38.97 (CH_2C(O)(N)CH_3, major), 35.47 ($C(CH_3)_3$), 33.74 ($BrCH_2$), 32.56 ($BrCH_2CH_2$, major), 32.52 ($BrCH_2CH_2$, minor), 29.38 (CH_2, major), 29.23 (CH_2, minor), 28.50 (CH_2), 29.47 (CH_2), 28.36 (CH_2), 27.81 (CH_2), 27.49 and 27.45 ($C(CH_3)_3$, major), 27.22 ($C(CH_3)_3$, minor), 24.40 (CH_2, minor), 24.04 (CH_2, major), 23.87 (RC-(O)(N)CH_3, minor), 19.46 (RC(O)(N)CH_3, major). FTIR (film) 2945, 2865, 1650, 1610, 1415 cm^{-1}; GC/CIMS (CH_4/NH_3(g)) m/z 376, 374 (MH^+). Anal. Calcd for $C_{18}H_{32}BrNO_2$: C, 57.75; H, 8.62; N, 3.74. Found: C, 57.81; H, 8.66; N, 3.69.

Methyl 3,4-Bis(7-(2*R*-methyl-3-acryloyl-4*S*-*tert*-butyl-2-oxazolidinyl)-heptyloxy)benzoate, *R*-16$_7$Bu. (2*R*,4*S*)-2-(7-Bromoheptyl)-2-methyl-3-acryloyl-4-*tert*-butyloxazolidine (420 mg, 1.12 mmol, 2.1 equiv), 89.7 mg (0.534 mmol, 1.0 equiv) of methyl 3,4-dihydroxybenzoate and 590.5 mg (4.27 mmol, 8.0 equiv) of anhydrous K_2CO_3 were mixed with 1.11 mL of DMSO and 2.60 mL of acetone and refluxed for 15 h. Upon cooling, the mixture was diluted with 20 mL of water and extracted with 3 × 25 mL of Et_2O. The pooled extracts were dried over $MgSO_4$, filtered, and condensed to a clear, light yellow oil. Flash column chromatography (25% EtOAc/hexane) followed by preparative normal phase HPLC (32.5% EtOAc/hexane) yielded 291.3 mg (72%) of a clear, colorless oil: TLC R_f 0.17 (25% EtOAc/hexane); ^{1}H NMR (300 MHz, $CDCl_3$) δ 7.62 (d of d, J = 8.4, 1.96 Hz, 1H; Ar-6-H), 7.52 (d, J = 1.96 Hz, 1H; Ar-2-H), 6.85 (d, J = 8.6 Hz, 1H; Ar-5-H), 6.53 (d of d, J = 16.6, 10.0 Hz, 2H; CH_2=CHR), 6.33 (d of d, J = 16.6, 1.9 Hz, 2H; HCH=CHR), 5.7–5.6 (m, 2H; HCH=CHR: 60 °C; δ 5.62, d of d, J = 10.0, 1.9 Hz, 2H), 4.42 (d, J = 6.4 Hz, 2H; NCH, minor rotational isomer), 4.05–3.85 (m, 8H; OCH_2), 3.87 (s, 3H; CO_2CH_3), 3.82–3.73 (m, 2H; NCH, major rotational isomer), 2.40–2.25 (m, 2H; diastereotopic HCHC(O)(N)-CH_3, major), 1.87–1.73 (m, 4H; OCH_2CH_2), 1.72 (s, 6H; RC(O)(N)-CH_3, major), 1.71 (s, 6H; RC(O)(N)CH_3, minor), 1.70–1.53 (m, 2H; diastereotopic HCHC(O)(N)CH_3, major), 1.50–1.18 (m, 16H; $O(CH_2)_2$-$(CH_2)_4$), 0.946 (s, 18H; *tert*-Bu, major), 0.915 (s, 18H; *tert*-Bu, minor). ^{13}C NMR (75 MHz, $CDCl_3$) δ 166.58 (CO_2,CH_3), 165.88 (C(O)N, minor rotational isomer), 164.53 (C(O)N, major rotational isomer), 152.83 and 152.76 (Ar), 148.11 and 148.07 (Ar), 130.56 (CH_2=CHR, major), 129.47 (CH_2=CHR, minor), 127.08 (CH_2=CHR, minor), 126.83 (CH_2=CHR, major), 123.23 (Ar-C-6), 122.08 and 122.02 (Ar), 113.88 and 113.83 (Ar-C-2), 111.56 (Ar-C-5), 98.05 (CH_2C(O)(N)CH_3, major), 95.73 (CH_2C(O)(N)CH_3, minor), 68.82 (4-OCH_2), 68.58 (3-OCH_2), 65.02 (ring OCH_2, major), 64.42 (NCH, major), 63.88 (NCH, minor), 63.83 (ring OCH_2, minor), 51.58 (CO_2CH_3), 39.38 (CH_2), 35.65 ($C(CH_3)_3$, minor), 35.57 ($C(CH_3)_3$, major), 34.54 and 34.51 (CH_2C-(O)(N)CH_3), 29.43 (CH_2), 29.25 (CH_2), 29.00 (CH_2), 28.89 (CH_2), 28.82 (CH_2), 28.77 (CH_2), 28.70 (CH_2), 27.40 and 27.35 ($C(CH_3)_3$, major), 27.08 and 27.04 ($C(CH_3)_3$, minor), 25.54 (CH_2), 24.03 (CH_2), 23.74 (RC(O)(N)CH_3); FTIR (film) 2940, 2865, 1715, 1650, 1605, 1415, 1290, 1270, 1215, 680 cm^{-1}. Anal. Calcd for $C_{44}H_{70}O_8N_2$: C, 69.99; H, 9.34; N, 3.71. Found: C, 70.05; H, 9.30; N, 3.71.

Methyl 3,4-Bis(7-((2*S*-methyl-3-acryloyl-4*S*-tert-butyl-2-oxazolidinyl)heptyl)oxy)benzoate, (*S*)-16$_7$Bu. (2*S*,4*S*)-2-(7-Bromoheptyl)-2-methyl-3-acryloyl-4-*tert*-butyloxazolidine (480 mg, 1.28 mmol, 2.1 equiv), 103.2 mg (0.614 mmol, 1.0 equiv) of methyl 3,4-dihydroxybenzoate and 692.4 mg (5.01 mmol, 8.2 equiv) of anhydrous K_2CO_3 were mixed with 1.28 mL of DMSO and 2.98 mL of acetone and refluxed for 15 h. Upon cooling, the mixture was diluted with 20 mL of water and extracted with 3 × 25 mL of Et_2O. The pooled extracts were dried over $MgSO_4$, filtered, and condensed to a clear, light yellow oil. Flash column chromatography (50% EtOAc/hexane) followed by preparative normal phase HPLC (45% EtOAc/hexane) yielded 330.6 mg (71%) of a clear, colorless oil: TLC R_f 0.32 (55% EtOAc/hexane); ^{1}H NMR (300 MHz, $CDCl_3$) δ 7.61 (d of d, J = 8.4, 1.96 Hz, 1H; Ar-6-H), 7.53 (d, J = 1.9 Hz, 1H; Ar-2-H), 6.84 (d, J = 8.5 Hz, 1H; Ar-5-H), 6.52 (d of d, J = 16.5, 10.0 Hz, 2H; CH2=CHR), 6.34 (d of d, J = 16.6, 2.1 Hz, 2H; HCH=CHR), 5.68–5.57 (m, 2H; HCH=CHR: 60 °C; δ 5.59, d of d, J = 10.1, 2.0 Hz, 2H), 4.40 (d, J = 5.0 Hz, 2H; NCH, minor rotational isomer), 4.07–3.85 (m, 8H; OCH_2), 3.86 (s, 3H; CO_2CH_3), 3.85–3.73 (m, 2H; NCH, major rotational isomer), 2.63–2.48 (m, 2H; diastereotopic HCHC(O)(N)-CH_3, major), 2.15–1.9 (m, 2H; CH_2C(O)(N)CH_3, minor), 1.90–1.65 (m, 4H; OCH_2CH_2 and m, 2H; diastereotopic HCHC(O)(N)CH_3, major), 1.50 (s, 6H; RC(O)(N)CH_3, major), 1.60–1.20 (m, 16H; $O(CH_2)_2$-$(CH_2)_4$), 0.930 (s, 18H; *tert*-Bu, major), 0.908 (s, 18H; *tert*-Bu, minor); ^{13}C NMR (75 MHz, $CDCl_3$) δ 166.61 (CO_2CH_3), 166.12 (C(O)N, minor rotational isomer), 164.73 (C(O)N, major rotational isomer), 152.83 (Ar), 148.11 (Ar), 130.59 (CH_2=CHR, major), 129.57 (CH_2=CHR, minor), 127.29 (CH_2=CHR, minor), 126.92 (CH_2=CHR, major), 123.26 and 123.21 (Ar-C-6), 122.01 (Ar), 113.88 and 113.80 (Ar-C-2), 111.56 (Ar-C-5), 97.97 (CH_2C(O)(N)CH_3, major), 95.64 (CH_2C(O)-(N)CH_3, minor), 68.86 (4-OCH_2), 68.61 (3-OCH_2), 64.83 (ring OCH_2, major), 64.38 (NCH, major), 63.82 (NCH, minor), 63.61 (ring OCH_2, minor), 51.59 (CO_2CH_3), 41.06 (CH_2C(O)(N)CH_3, minor), 38.99 (CH_2C(O)(N)CH_3, major), 35.44 ($C(CH_3)_3$), 29.59 (CH_2), 28.95 (CH_2), 28.84 (CH_2), 28.72 (CH_2), 27.41 ($C(CH_3)_3$, major), 27.18 ($C(CH_3)_3$, minor), 25.59 (CH_2), 25.52 (CH_2), 24.45 (CH_2, minor), 24.08 (CH_2), 23.82 (RC(O)(N)CH_3, minor), 19.42 (RC(O)(N)CH_3, major); FTIR (film) 2940, 2865, 1715, 1650, 1605, 1415, 1290, 1270, 1220, 680 cm^{-1}. Anal. Calcd for $C_{44}H_{70}O_8N_2$: C, 69.99; H, 9.34; N, 3.71. Found: C, 69.88; H, 9.36; N, 3.65.

Isolation of telomer 10 (n = 2, R = allyl). The ethereal solution of telomers from a 2.5^A/80^l/200^{Sn} ACT reaction run on 108 mg (0.144 mmol) of (*R*)-16$_7$Bu was condensed under vacuum and purified by flash column chromatography (5% EtOAc/hexane) to yield 12 mg (0.041 mmol, 28%) of clear oil **10** (n = 2, R = allyl) as a 23:1 mixture (GC analysis): TLC (5% EtOAc/hexane) R_f 0.15, (10% EtOAc/hexane) R_f 0.29, GC (1 min at 80–300 °C at 15 °C/min) t_R 9.02 (minor), 9.19 (major) min GC/CIMS (CH_4/NH_3(g)) m/z 297 (MH^+); ^{1}H NMR (300 MHz, $CDCl_3$) δ 5.71 (d of d of t, J = 15.6, 10.2, 7.0 Hz, 1H), 5.05 (d of d, J = 15.6, 1.5 Hz, 1H), 5.03 (br d, J = 10.1 Hz, 1H), 3.67 (s, 3H), 3.66 (s, 3H), 2.56–2.20 (series of m, 4H), 1.96 (d of t, J = 13.9, 8.0 Hz, 1H), 1.80–1.48 (series of m, 7 H), 1.34–1.05 (series of m, 5H), 0.96–0.73 (m, 2H) ppm; ^{13}C NMR (75 MHz, $CDCl_3$) δ 176.37, 175.34, 134.83, 117.19, 51.55, 43.13, 40.67, 40.00, 36.14, 35.48, 34.22, 33.61, 32.68, 26.45, 26.15, 26.12 ppm. Anal. Calcd for $C_{17}H_{28}O_4$: C, 68.88; H, 9.54. Found: C, 68.70; H, 9.55.

Isolation of Macrocycles and n = 4 Precursors. A benzene stock solution of covalent assembly (*R*)-16$_7$Bu (17.4 mL, 101 mg, 0.134 mmol) was mixed with 32.4 mL of benzene, 555 μL (0.901 g, 4.29 mmol, 31.9 equiv) of cyclohexyl iodide, and 3.33 mL (3.56 g, 10.7 mmol, 80.0 equiv) of allyltri-*n*-butylstannane. After purging the solution 0.5 h with argon, 4.6 mg of AIBN was added, and the mixture brought to a gentle reflux using an 85 °C oil bath. After 2 h, another 4.1 mg of AIBN was charged into the reaction mixture, and reflux continued another 14 h before being allowed to cool to room temperature. Benzene was removed under vacuum, and the residual liquid (~4 mL) was distilled under high vacuum (75–78 °C at 0.002 mmHg) to remove the bulk of the tin compounds. The oily pot residue was stirred overnight with 25 mL of ether and 25 mL of 10% (w/w) aqueous KF solution, and the layers separated. The ether layer was dried over $MgSO_4$, filtered, and condensed to an oil that was purified by flash column chromatography (25% EtOAc/hexane) to give 53.1 mg of a mixture of macrocycles. An additional 18.1 mg of macrocycle was isolated from the early (15% EtOAc/hexane at 10.0 mL/min, elution time 22.2 min) and late (25% EtOAc/hexane at 10.0 mL/min, elution time 12.1 min) eluting fractions by preparative normal phase HPLC. The total isolated weight was 71.2 mg (0.081 mmol, 60%): TLC (25% EtOAc/hexane) R_f 0.36; ^{1}H NMR (300 MHz, $CDCl_3$) δ 7.68–7.59 (m, 1H), 7.56–7.48 (m, 1H), 6.87–6.80 (m, 1H), 5.92–5.60 (m, 1H), 5.14–4.97 (m, 2H), 4.36–4.28 (m, 1H), 4.14–3.55 (series of m, 9H), 3.86 (s, 3H), 2.82–1.94 (series of m, 6H), 1.9–0.8 (series of m and s, 61 H) ppm.

While obtaining additional macrocycle via HPLC purification of the late eluting flash column fractions, 8.0 mg (7%) of material was collected whose ^{1}H NMR was consistent with structures having two templates incorporated in bismacrocyclic compound. The material was subjected to the standard assay as described earlier, and the resulting telomer distribution was determined to be **10** (R = allyl): n = 1, 8.1$_5$%; n = 2, 2.3$_7$%; n = 3, 1.7$_1$%; n = 4, 87.$_8$%.

Preparation of Diamides Bis(*N*-1*S*-phenylethyl)-2*S*-(cyclohexylmethyl)-4-(2-propenyl)-1,5-pentanedicarboxamide, 19a–d. 1-(Cyclohexane)hept-6-ene-2,4-dicarbonyl chloride, 0.43 g (1.4 mmol), was combined with 7.0 mL of dry benzene in a flame dried flask. Pyridine (0.24 mL, 3.0 mmol), and 0.40 mL (3.0 mmol) of (*S*)-(−)-α-methylbenzylamine (Aldrich, 98%) were added. A $CaSO_4$ drying tube was affixed, and the mixture was stirred at room temperature for 3 h. The reaction mixture was diluted with 100 mL of EtOAc and washed with 3 × 20 mL portions of H_2O and 20 mL of saturated brine solution. The organic layer was dried over anhydrous $MgSO_4$, and the EtOAc was removed in vacuo to give 0.54 g of light brown solid: GC (SPB-1, 15 m, 5 psi; 100 °C for 1 min, 15 °C/min to 280 °C) 16.5 min (25%), 17.2 min (25%), 17.5 min (14%), 17.7 min (13%); (SPB-5, 30 m, 15 psi; 200 °C for 5 min, 15 °C/min to 280 °C) 30.4 min (19%), 33.7 min (20%), 34.2 min (15%), 35.6 min (14%). The *erythro* isomers were separated from the *threo* isomers based on their increased solubility in 20% EtOAc:80% hexanes. Each of the individual isomers was isolated by column chromatography (Si, 85% $CHCl_3$:15% EtOAc).

19a: R_f 0.80 (Si, 85% $CHCl_3$:15% EtOAc); ^1H NMR (300 MHz, $CDCl_3$) δ 7.2–7.4 (m), 6.1 (m), 5.6 (m), 4.9–5.3 (m), 2.0–2.4 (m), 1.7 (m), 1.5 (m), 1.25 (m), 1.15 (m), 0.7–1.0 (m); ^{13}C NMR (300 MHz, $CDCl_3$) δ 174.45, 173.41, 143.52, 143.38, 135.33, 128.86, 128.81, 128.60 (weak), 127.84 (weak), 127.77, 127.59, 127.29 (weak), 126.60, 126.55, 126.25 (weak), 116.76, 46.95, 46.85, 45.36, 42.58, 40.91, 37.33, 37.16, 35.43, 33.69, 32.83, 29.73, 26.49, 26.22, 19.45, 19.37; IR (CCl_4) 3424 (w), 3403 (w), 3007 (m), 2927 (s), 2852 (w), 1663 (s), 1507 (s), 1450 (w), 920 (w) cm^{-1}; GC/MS (EI) *m/z* calcd for $C_{31}H_{42}N_2O_2$: 474.3249, found 474.3230.

19b: R_f 0.62 (Si, 85% $CHCl_3$:15% EtOAc); ^1H NMR (300 MHz, $CDCl_3$) δ 7.6 (m), 7.2–7.4 (m), 5.75 (m), 5.05 (m), 1.8–2.5 (m), 1.6 (m), 1.5 (m), 1.25 (m), 1.05 (m), 0.6–1.0 (m); IR (CCl_4) 3434 (w), 3008 (m), 2927 (s), 2852 (w), 1662 (s), 1505 (s), 1450 (m), 925 (w) cm^{-1}; GC/MS (EI) *m/z* calcd for $C_{31}H_{42}N_2O_2$: 474.3249, found 474.3227.

19c: R_f 0.39 (Si, 85% $CHCl_3$:15% EtOAc); ^1H NMR (300 MHz, $CDCl_3$) δ 7.6 (m), 7.2–7.4 (m), 5.75 (m), 5.05 (m), 1.8–2.5 (m), 1.6 (m), 1.5 (m), 1.25 (m), 1.05 (m), 0.6–1.0 (m); IR (CCl_4) 3433 (w), 3007 (m), 2927 (s), 2852 (w), 1664 (s), 1502 (s), 1450 (m), 920 (w) cm^{-1}; GC/MS (EI) *m/z* calcd for $C_{31}H_{42}N_2O_2$: 474.3249, found 474.3251. X-ray crystallographic analysis established the absolute configuration as (2*R*,4*S*).

19d: R_f 0.26 (Si, 85% $CHCl_3$:15% EtOAc); GC/MS (EI) *m/z* calcd for $C_{31}H_{42}N_2O_2$: 474.3249, found 474.3245. It was not possible to isolate enough of the pure isomer to obtain NMR or IR spectroscopic data.

Conversion of ACT Products to Diamides 19. The mixture of methyl esters derived from the ACT reaction, 22.0 mg, was combined with 2.0 mL of a 2.8 N KOH solution (1/1 EtOH/H_2O) and gently refluxed for 6 h. The reaction mixture was concentrated under reduced pressure. The residue was dissolved in 10 mL of EtOAc and washed with 2 × 10 mL portions of 1 N HCl. The organic layer was dried over anhydrous $MgSO_4$ and concentrated in vacuo. The resulting brown oil was dissolved in 2.0 mL of dry benzene in a flame dried flask. Oxalyl chloride, 0.08 mL, was added, and the mixture was stirred at room temperature for 20 min and then gently refluxed for 2 h. Excess oxalyl chloride was removed in vacuo, and the resulting oil was dissolved in 3.0 mL of dry benzene. Pyridine, 20.0 μL (3.2×10^{-7} mol), was added followed by 50 μL (4.0×10^{-7} mol) of (*S*)-(−)-α-methylbenzylamine. A $CaSO_4$ drying tube was affixed, and the mixture was stirred at room temperature for 4 h. The reaction mixture was diluted with 20 mL of EtOAc and washed with 3 × 10 mL portions of H_2O and 10 mL of saturated brine solution. The organic layer was dried over anhydrous $MgSO_4$, and the EtOAc was removed in vacuo to give ca. 10.0 mg of an oily yellow solid: GC (SPB-5, 30 m, 15 psi; 200 °C for 5 min, 15 °C/min to 280 °C) 30.4 min (6%), 32.5 min (1%), 33.2 min (9%), 34.0 min (84%). Only the relative ratios of the diamide isomers are reported. The retention time of the major isomer was verified by coinjection with an authentic sample.

X-ray Crystal Structure Analysis of 14 and 19c. Crystal data: **14**, $C_{14}H_{25}NO_3$, M = 255.36, monoclinic, space group $P2_1$, a = 9.571(1) Å, b = 9.794(1) Å, c = 8.783(1) Å, β = 112.76(1)°, V = 759.2(3) Å^3, Z = 2, D_{calcd} = 1.117 g cm^{-3}, μ(Cu Kα) = 5.9 cm^{-1}; **19c**, $C_{31}H_{42}N_2O_2$, M = 474.69, tetragonal, space group $P4_12_12$, $a = b$ = 19.410(3) Å, c = 15.899(1) Å, V = 5990(3) Å^3, Z = 8, D_{calcd} = 1.053 g cm^{-3}, μ(Cu Kα) = 4.7 cm^{-1}.

Intensity data from both crystals [$+h,-k,\pm l$; θ_{max} = 75°, 1645 nonequivalent reflections for **14**; $+h,+k,+l$; θ_{max} = 57°, 2343 nonequivalent reflections for **19c**] were recorded on an Enraf-Nonius CAD-4 diffractometer [Cu Kα radiation, λ = 1.5418 Å; graphite monochromator; ω-2θ scans, scanwidth (1.00 + 0.14tan θ)°]. Refined unit-cell parameters were derived in each case from the diffractometer setting angles for 25 reflections (35° < θ < 40°) widely separated in reciprocal space. Both crystal structures were solved by direct methods (MULTAN11/82). Full-matrix least-squares adjustment of positional and thermal parameters (anisotropic C, N, O; isotropic H for **14**, calculated H for **19c**) converged (max. shift:esd = 0.03) at R = 0.040 (R_w = 0.056) for **14** and R = 0.083 (R_w = 0.102) for **19c** over 1259 and 1432 reflections, respectively, with $I > 3.0\sigma(I)$. Further details of the analysis are summarized in the supplementary material.[25] Crystallographic calculations were performed on PDP11/44 and MicroVAX computers using the Enraf-Nonius Structure Determination Package (SDP 3.0). For structure-factor calculations, neutral atom scattering factors and their anomalous dispersion corrections were taken from ref 26.[26]

Acknowledgment. This research was supported by grants from NSF and NIH (HL 17921). G.S.M. acknowledges a Tennessee Eastman Fellowship and R.L.C. acknowledges NIH for a postdoctoral fellowship.

Supplementary Material Available: Tables of crystallographic data, atomic positional and thermal parameters, bond lengths, bond angles, torsion angles, and hydrogen-bonded distances for **14** and **19c** (17 pages). This material is contained in many libraries on microfiche, immediately follows this article in the microfilm version of the journal, and can be ordered from the ACS; see any current masthead page for ordering information.